Development of Oral Influenza Vaccine Delivery System Utilizing pH Responsive Pored Microparticles

by

Ankit Kumar

A thesis submitted in partial fulfillment of the requirements for the degree of

Master of Science

in

Chemical Engineering

Department of Chemical and Materials Engineering
University of Alberta

Abstract

Influenza is a major respiratory disease caused by influenza virus. Recent spread of the extremely pathogenic avian and swine influenza viruses paint a morbid picture of the emergence of a more lethal influenza virus in future. Currently, hypodermic needles are being dominantly employed in vaccination worldwide. However, inherent limitations such as the need for highly skilled healthcare workers, high cost (production and administration), and safety concerns over needle reuse render it undesirable in developing nations. As an alternative, solid oral vaccines have emerged as a promising platform due to potential advantages like generation of both mucosal and systemic humoral immune responses, no biohazardous waste (i.e., needles), no prerequisite for cold supply chain for transportation/storage, convenient stockpiling due to solid formulation, long shelf life, and the ability to self-administer. Despite these potential advantages of oral vaccines, they are still elusive to commercialization due to their instability in the gastric environment. Our research goal is to develop a novel oral vaccine delivery vehicle, which can sense pH change of the environment. To this end, we successfully fabricated a Microparticle-based vaccine delivery system, which can protect and release vaccines in response to different pH environments of the stomach and small intestine, respectively. In this research, comprehensive methodology to fabricate microparticles has been reported. As a systematic approach, concept testing was

performed to identify any potential design problems or challenges associated with MPs prior to their incorporation of real vaccine. Briefly, MPs were synthesized in oil-in-water (O/W) emulsion method using Poly (methyl methacrylate) (PMAA)-based Food and Drug Administration (FDA) approved anionic copolymer. Combined effects of temperature and solvent composition/evaporation conditions on MPs characteristics were investigated to find key process parameters to make optimally functioning pH-responsive MPs. Morphological change of the MPs was shown to be important to maintain high level of antigenic stability from *in vitro* experiments using model drugs (100 nm polystyrene nanoparticles and sulforhodamine b). Morphology and size of MPs were examined with scanning electron microscopy (SEM) and dynamic light scattering (DLS) at gastric/intestine pH conditions. Quantitative analysis of the loading efficiency and time dependent release profile of model drugs were performed using a plate reader and fluorescence microscope. Furthermore, for detailed surface characterization of MPs, FTIR, NMR and DSC analysis were performed. Although these efforts were majorly aimed at the demonstration of concept *in vitro*, this work is expected to contribute to development of a universal platform for oral vaccines.

Acknowledgement

I would like to express my deepest appreciation to Dr. Carlo Montemagno and Dr. Hyo-Jick Choi, my supervisors. Dr. Montemagno has been a beacon of inspiration to me right from the start. Whenever I was lacking motivation or failing in experiments, he convinced me to keep my resolve intact and to believe in my capabilities, which sometimes were all that kept me going. He taught me to envision the big picture of my research, which helped me immensely in planning and executing experiments without any major setbacks.

I cannot express enough gratitude to Dr. Choi for his constant guidance and unwavering support. He not only shaped this project right from its inception to the conclusion, but also molded my overall outlook towards research. He personally made efforts in teaching me relevant laboratory related skills, and in providing valuable guidance at every juncture of this project. He provided me with multitude of opportunities to improve my research skills as well as my overall personality. Also, his advice on life in general, is something I would always remember.

I would like to thank my colleague, Chengmeng Sun for helping in obtaining model drugs' release data. Also, I would like to thank Ingenuity Lab members, and NINT for providing support and vital instruments.

I am also grateful to my close friends especially, Andrew Jo, Ankit Singh, Deepesh Kumar, Pankaj Agarwal, and Sahil Bangar for always being supportive and encouraging.

Lastly, I would like to thank my family (Dad, Mom, and Anupam) for their unconditional love and support.

Table of Contents

Table of Figures

1 Introduction

Drug delivery systems have advanced quite a great deal in past few decades. With the advent of controlled drug delivery, drugs can now be delivered to a particular site of interest with tunable release behavior. Unfortunately, development of oral vaccines has been challenging because of destabilization of biomolecules such as proteins, peptides, and antigens in gastric and enzyme rich environment of the stomach[1]. With the looming threat of influenza epidemic/pandemic, lack of effective preventive measures and ineffectiveness of current immunization choices, development of a potent alternative is a must. In this section, first the background of influenza and the currently employed strategies are discussed, followed by the overview of global research efforts in this field, and finally our proof-of-concept novel vaccine delivery system is introduced as the first step in solving this serious predicament.

1.1 Influenza

Influenza viruses are enveloped, single-stranded RNA viruses, which belong to the Orthomyxoviridae family[2] (Figure 1.1). They have been responsible for major epidemic and pandemic respiratory diseases worldwide with substantial morbidity

and mortality. They account for more than 250,000 deaths per year worldwide, posing a significant economic burden on the healthcare expenses[3]. In the U.S. alone, influenza epidemics lead to more than $80 billion dollars annually in healthcare expenditure[4]. Recent spread of an extremely pathogenic H5N1 avian influenza virus (2003) and a swine originated H1N1 influenza virus (2009) paint a grim picture of the emergence of a more lethal influenza virus in the near future[5,6]. Outbreak of an influenza pandemic is inevitable in the near future. Simulations conducted for even a moderate level of influenza outbreak have indicated a staggering expenditure of nearly $181 billion in damages, which could potentially destabilize a country's economy and its security interests[7]. Given the possibility of a future outbreak of these lethal viruses and the impending danger presented by them, it is of paramount importance to develop an efficient strategy for combating these viruses. Fortunately, vaccination has been widely recognized as the most efficient strategy to combat continuing threat of influenza pandemic[8].

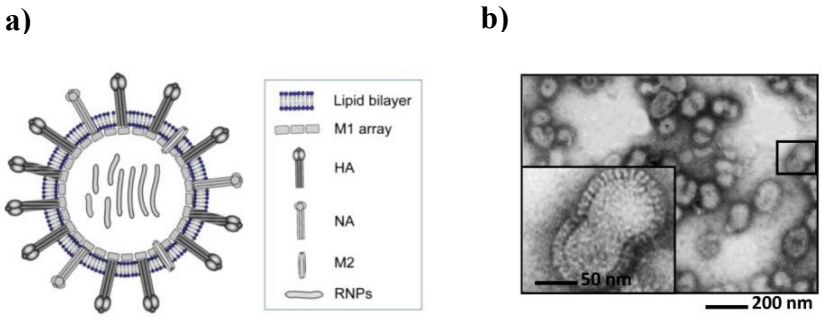

Figure 1.1 a) Structure of influenza virus and b) TEM micrograph of formaldehyde-inactivated A/PR/8/34 influenza virus[51]

1.2 Current vaccinations and their disadvantages

Currently, intramuscular (IM), intradermal (ID), and intranasal (IN) administration are the available licensed methods for influenza vaccination[9]. Hypodermic needles are being dominantly employed in universal mass vaccination[10]. However, various studies have reported the incomplete protection ranging from 30-90% is provided by injected vaccines[11]. Moreover, the administration of these needles strongly necessitate the availability of highly skilled healthcare workers, thereby limiting their usage in developing countries[12]. In addition, other complications associated with these needles such as the proper disposal of biohazard waste, needle related injuries and diseases caused by improper needle reuse, render it undesirable choice for global vaccination[13,14]. Other major drawbacks of the current influenza vaccines include their time-consuming manufacturing process, which is attributed to their production through hen's egg-based system and their requirement of refrigerators for storage[15,16]. Also, current vaccine stockpile will become inefficient by the emergence of a new strain, which is almost always the case due to the ever-changing conformations of the virus. It has been estimated that new strain vaccine production process would take at least 4-6 months, while mathematical simulations have predicted that a pandemic influenza will require only 6 months to spread throughout the world. Moreover, the current vaccine production capacity is only 3

billion doses per year, substantially short of the 6.8 billion people who will be at risk of contracting influenza[17].

IN administration with the live attenuated influenza vaccine is a mucosal vaccination method available for use for healthy people in the age group of 5–49 years in the US[9]. Despite having several advantages including its ability to induce mucosal and systemic immune responses together, IN vaccines have safety concerns over the potential formation of facial paralysis called Bell's palsy[18,19]. This has led to an extensive research on the development of alternative vaccine delivery methods and formulations. Especially, oral influenza vaccine has gained major traction in the scientific community due to their unique advantages.

1.3 Oral vaccine and Technical challenges

Oral vaccines provide a promising platform for helping people in developing countries as well as for the preparation of pandemic influenza. This can be attributed to their several potential advantages: no necessity for the disposal of biohazardous waste since needles are not required for vaccination, cost-effectiveness as there is no prerequisite for cold supply chain for transportation, and dose sparing technology[10,12]. Moreover, they do not require highly trained personnel as the final product will be an easy-to-take pill. Also, stockpiling will be

much easier since the vaccine will be in solid formulation with higher shelf life. Oral vaccines after ingestion are recognized by Microfold (M) cell in the Peyer's patches of the intestine and by dendritic cells that are present there[1]. Additionally, they can induce both systemic and mucosal immune responses, hence, providing improved defense at ports of entry for viruses[20].

Although considerable efforts have been devoted towards the development of oral influenza vaccines, oral influenza vaccines are commercially unavailable. From *in vivo* animal studies, it has been demonstrated that an orally administered influenza vaccine does not produce satisfactory levels of immunogenicity as compared to other routes of administration because of the destabilization of oral vaccines in the stomach[21,22]. Therefore, to induce a similar level of protective immunogenicity, the vaccine must contain a larger quantity of antigens resulting in the decrease of economic benefits of inactivated oral influenza vaccine[23]. To overcome this issue, the use of strong adjuvants such as the bacterial enterotoxins have been successfully reported[24]. However, most of the enterotoxins are toxic to humans, and hence cannot be used[25].

Of the various approaches explored by scientists to overcome the technical challenges posed by oral vaccines, microparticle-based drug delivery approaches are discussed in the next section.

1.4 Microparticle based delivery approaches

1.4.1 Microparticles, utilities, and release mechanism

Spherical particles which range in size from 1 μm to 1000 μm have been classified as microparticles (MPs)[26]. With flexibility in choice of material for preparing them, MPs have been utilized in a wide range of applications. Polymeric MPs have a continuous phase, which has particulate drug dispersed throughout the polymer matrix[27]. Polymer degradation and polymer erosion come under release mechanisms for drugs entrapped into MPs. Polymer degradation is caused by chemical reactions, which cleave the main-chain bonds of a polymer, in turn, producing shorter chain oligomers and monomers. During this process, side products are also generated which have lower molecular weight. If this phenomenon is attributed to biocatalytic processes initiated by bacteria or enzymes, or by chemical and radical processes such as hydrolysis or oxidation, then the polymer is classified as biodegradable. Biodegradable polymers have generated huge interests in scientific community, and have been widely researched with applications in packaging, agriculture, and in drug delivery devices. In case of erosion, it can occur either at surface level or at bulk level depending on the extent of water transportation through them[28].

Another way to trigger drug release is by utilizing the stimuli responsive polymers. These polymers respond to external stimuli such as pH milieu[29], temperature[30], light[31], and magnetic field[32] amongst many more. Due to this particular behavior, they are also termed as smart or intelligent polymer[33,34]. Much focus has been given to the polymers which respond to pH (pH sensitive or pH responsive polymer), due to the fact that gastrointestinal (GI) tract of humans has variable pH throughout its length[35], hence making them an ideal candidate for targeted delivery such as in colon.

1.4.2 Conventional MPs based vaccine delivery approach

After oral ingestion of vaccines, it must pass through the harsh acidic environment of the stomach to reach the small intestine where it's taken up by the intestinal cells present in the epithelium of Peyer's patch for generating appropriate immune responses. MPs present unique advantage in terms of their absorption from the intestine through Peyer's patches- making them an apt delivery carrier for oral immunization[36]. Vaccines are extremely sensitive to external environment and might denature in the harsh environment of GI tract[23]. Fortunately, it has been reported that the polymer walls protect the vaccine from the harsh gastric environment of the stomach (low pH), and the proteolysis in the gut[37]. MPs prepared from various materials PLGA[38], PLA[39], PCL[40], chitosan[41] have already

been documented for vaccine delivery. Particularly for influenza vaccines, different approaches have been explored[42,43]. But the use of organic solvents in preparation of MPs, and the inevitable contact of vaccines with them, result in the loss of activity of vaccines and also raise safety concerns. Shastri et al. proposed solution for this by preparing MPs from water soluble polymers using spray drying technique[44]. However, spray drying technique has major disadvantage due to high operating temperature, which might damage the thermo-sensitive drugs[45], such as influenza vaccine, which loses efficacy at high temperatures[23]. Therefore, a new approach must be proposed for overcoming all the technical hurdles faced by conventional MPs based delivery systems- problems associated with contact between influenza vaccine and organic solvent, and the activity loss of the vaccine due to high temperatures, for developing a MP-based influenza vaccine.

1.4.3 Novel delivery system design

As mentioned above, there are several technical hurdles which need to be considered for a novel efficient delivery system for influenza vaccines. If the delivery system is MP-based then technical challenges include: 1) selection of an already existing biocompatible polymer which is approved for clinical application by FDA as developing a new polymer and getting approval from FDA will unnecessarily increase the timeline for its commercial use; 2) fabrication & quality

control over MPs i.e., size, polydispersity, yield, and simple process for mass production. MPs with size < 21 μm have been reported to taken up effectively by M cells[46], which might enhance the effectiveness of delivery system; 3) design of MPs for optimal vaccine loading efficiency and stabilization in acidic gastric environment, and rapid release in small intestine; 4) development of formulation to stabilize vaccine during drying process as the conformational change of antigens due to dehydration would reduce their efficacy.

Our proposed delivery system comprises of all the advantages that are needed to counteract the aforementioned technical challenges. Pored MPs are fabricated by utilizing a modified oil-in-water emulsion solvent evaporation technique. The MPs are made up of an anionic pH sensitive polymer, which has been approved by FDA for drug application. The presence of pores on MPs' surface allow easy loading of vaccines into them. Due to pH sensitive property, the pores once closed remain unchanged in gastric environment, and open in the neutral environment of intestine to facilitate rapid release of vaccines, which are subsequently absorbed by intestinal cells to generate appropriate immune responses (Figure 1.2).

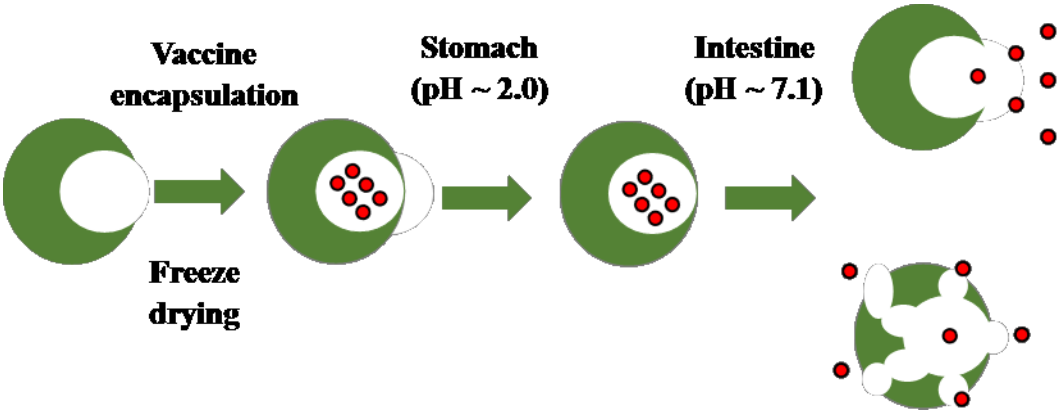

Figure 1.2 Schematic representation of proposed delivery system

To successfully complete this research work, it was divided into multiple research goals as follows:

1. Fabricate MPs with macropores capable of protecting vaccines at low pH and facilitating a rapid release of vaccines at neutral pH.
2. Develop a technique to close the macropores efficiently.
3. Assess feasibility of delivery system in simulated GI tract environment.
4. Demonstrate the proof-of-concept of vaccine delivery system *in vitro* by encapsulating model drugs and investigating their release behavior.
5. Examine the recyclability behavior of vaccine delivery system.

2 Materials and Methods

2.1 Materials

All chemicals were used as received unless otherwise specified. EUDRAGIT® S 100 (abbreviated as S100) polymer used for MPs preparation was received as a generous gift from Evonik Canada Inc. (Burlington, Ontario, Canada). For preparation of aqueous phase in O/W emulsion, and for all other experiments wherever water was needed, 0.2µm filtered deionized (DI) water was used. Aqueous phase emulsifier- Poly (vinyl alcohol) (PVA), Mw: 9000-10,000, and detergent-Tween™ 20 (abbreviated as Tween 20), Fisher BioReagents™, were purchased from Sigma-Aldrich (St Louis, Missouri, USA) and Fisher Scientific (Missisauga, ON), respectively. Co-solvent system used in oil phase were Ethanol (Sigma–Aldrich), and Dichloromethane and Isopropanol (Fisher Scientific). For making homogenous emulsions, GE-130 ultrasonic processor from Sonics & Materials, Inc. (Newtown, Connecticut, USA) was used. Benchtop centrifuge (Eppendorf™ Model 5810) was utilized during washing of MPs and for concentrating the samples. Büchi® R200 rotary evaporator was used for removal of remaining solvents from MPs. Whatman® qualitative filter paper (grade 4) were utilized for separating MPs less than 20 µm. AdVantage Pro Freeze Dryer was used

for lyophilization and pore closure purposes. Sulforhodamine B (Dye content 75 %) used for encapsulation was from Sigma-Aldrich. Fluorescent nanoparticles (abbreviated as FNP; FluoSpheres® Carboxylate Microspheres, 0.1 μm) were purchased from Life Technologies.

2.2 Fabrication of MPs with a macropore

2.2.1 General Technique

A new and simple method was developed to make MPs with macropores using modified O/W emulsion solvent evaporation method. In a typical synthesis procedure, 5 wt% S100 polymer is dissolved in the co-solvent system (Dichloromethane: Ethanol: Isopropanol = 2:1:1) to prepare oil phase. It is then added into an aqueous phase of DI water containing 0.5% PVA as an emulsifier and 5% Tween 20 as a detergent to make O/W emulsion by applying sonication at 30 W. Post sonication, emulsion was stirred at room temperature (R.T.) for 3 hrs, and the mixture was washed with water four times via centrifuge (12,000 g, 20 min). The concentrated residue suspension was rotary evaporated to remove remaining solvents (65°C, 5-10 min) in the particles. Afterwards, the final suspension was vacuum filtered using Whatman® filter papers (Grade 4) to collect MPs (< 20 μm). Filtered samples were concentrated and freeze dried for further analysis.

2.2.2 Study of different sonication methods on emulsion temperature, stability, and MPs properties

To control the evaporation rate of solvent from MPs, multiple process conditions were tested including sonication time, sample volume (50 ml, 100 ml, and 200 ml), sonication methods (continuous, discontinuous), and emulsion temperature control (R.T. sonication, iced water sonication), Specifically, the sample temperature was compared for two different sonication methods: continuous sonication (sonication cycle on throughout), and discontinuous sonication (sonication cycle on 5 min, off for 10 min and then on for 5 min – this continued for a specified time interval) with two different sample conditions- 1) unrefrigerated (no external temperature control, i.e. R.T. sonication), and 2) refrigerated samples (iced water to control the sample temperature, i.e. iced water sonication for varying total sonication time durations (5, 10, 15, 30, and 60 min). Post incubation, MP containing emulsion was washed with DI water four times via centrifuge (12,000 g, 20 min) and rotary evaporated (65°C, 5-10 min). Afterwards, the final suspension was filtered using 20 μm filter papers, concentrated using centrifugation, and freeze dried for SEM and DLS characterization.

2.2.3 Study of slow solvent evaporation on MPs

In case of R.T. stir incubated MPs, 5 wt% S100 polymer is dissolved in the co-solvent system (Dichloromethane:Ethanol:Isopropanol = 2:1:1) and added into an aqueous phase of DI water containing 0.5% PVA and 5% Tween 20- to make O/W emulsion by applying sonication (30 W, 5 min) at R.T.. For the IW stir incubated MPs, the emulsion is prepared in a similar manner but the sonication is applied under iced water condition (container was surrounded by iced water). In both cases, sonicated emulsion was further magnetically stirred (700 rpm) at R.T. for a specified time interval (0, 2, 4, and 8 hrs), followed by centrifuge washing (12,000 g, 20 min) and rotary evaporation (65°C, 5-10 min). Samples were filtered, concentrated, and freeze dried as previously described for further characterization.

2.2.4 Preparation of MPs for encapsulation and pH responsiveness tests

In all the three types of MPs (30-10-30, R.T., and IW), the emulsion preparation process parameters and purification protocol were same as described in general technique (see section 2.2.1). However, the only difference was in terms of sonication and incubation condition: for 30-10-30 MPs, emulsion was sonicated for a cycle of 30 min on-10 min off- 30 min on; for R.T. MPs, emulsion was sonicated for 5 min at R.T. condition followed by magnetic stir (700 rpm) at R.T. for 4 hrs;

for IW MPs, emulsion was sonicated for 5 min at iced water condition followed by magnetic stir (700 rpm) at R.T. for 4 hrs.

2.3 Pore closure by freeze drying

To close pores of MPs, a new method was developed using freeze dryer. Initially, concentrated MPs suspension in water was stored in a 2 ml Eppendorf tube and then frozen using liquid nitrogen. After that, it was transferred to freeze dryer, which was already pre-cooled to -40°C. MP samples were freeze-dried using a recipe, which was formulated considering polymer properties and co-solvent system (see Table 2-1). Samples were stored in 4°C refrigerator after collection.

Table 2-1: Recipe for freeze drying

Step	Shelf (°C)	Ramp (min)	Hold (min)	Vacuum (mTorr)
Primary Drying				
1	-40	0	30	1000
2	-55	60	1	100
3	-55	0	2000	100
Secondary Drying				
4	30	180	120	300

2.4 pH responsiveness of MPs

To test pH responsive behavior of MPs, samples were subjected to two kinds of buffers – acidic and neutral. Acidic buffer having a pH 2.0 was prepared using a potassium chloride (KCl)/hydrochloric acid (HCl) buffer. In a typical method, 0.1 wt% KCl solution was kept on a magnetic stirrer plate, and then 0.1 wt% HCl was added dropwise to adjust the final pH to be 2.0. To prepare neutral pH buffers, 0.1 wt% disodium phosphate (Na_2HPO_4) was added dropwise to KCl/HCl acidic buffer until the final pH reached to 7.1.

A small amount of lyophilized MPs powder was suspended in acidic buffer, and then the sample was incubated for 2 hrs at 37°C in oven to simulate gastric environment. Half of the sample was collected for further characterization, and the rest half was mixed with 0.1 wt% disodium phosphate to make the final pH 7.1, which corresponds to the intestine pH. It was incubated for further 4 hrs to simulate intestine digestion time. Final sample was collected for further SEM and DLS characterization.

2.5 MPs freeze-drying cycle tests

Multiple cycles (1, 3, 5, and 10 cycles) using the recipe mentioned in section 2.3 were carried out with the same batch of sample. For example with respect to total number of cycles 3, initially the concentrated MPs suspension in water was subjected to a freeze drying cycle as described in section 2.3 to close the pores. Then, the samples were taken out and resuspended in DI water to open the pores, and refrozen using liquid nitrogen and subjected to another freeze drying cycle, which makes it a total of 2 freeze drying cycle. Again, after the cycle was completed, samples were collected and resuspended in DI water to open the pores and subjected to another freeze drying cycle, completing the third, and in this example, final cycle. Before the start and after the finish of an above specified freeze drying cycle, samples were collected for SEM and DLS characterization.

2.6 Dye/FNP encapsulation/release experiments

2.6.1 Dye/ FNP encapsulation

1ml DI water was transferred to a 2 ml tube containing already freeze-dried and weighed MPs powder. Two more tubes were prepared in similar way for replication purposes. These samples were centrifuged at 10,000 rpm for 10 minutes. After centrifuge, the supernatant was removed and remaining MP pellet was suspended in 300 µl of 300 mM trehalose in DI water, and 10 µl of 50-times diluted SB solution (1 ml SB in 50 ml DI water). Similarly, in case of FNP, pellet was suspended in 1 ml of 100 nm nanoparticles solution, which was diluted 5 times from the original in 300 mM trehalose in DI water. All samples were put into vacuum oven with vacuum on/off cycle for 4~5 times. This ensured that all the air pockets were removed from pored MPs and are replaced by dye/FNP. After that, it was centrifuged at 10,000 rpm for 10 min to remove the external dye which is not encapsulated in MPs. A 1 ml micro-pipette was used to remove major supernatants and then a 100 µl micro-pipette was employed to remove remaining supernatants. Then 1 ml of DI water was added to the each tube and it was quickly vortexed for 1~2 s and cooled with liquid nitrogen. Then all cooled samples were freeze dried with the help of freeze dryer by employing the same recipe as mentioned in section 2.3.

2.6.2 Dye/ FNP release

Upon completion of freeze drying process, samples were collected and weighed again. Then, a known amount of sample, which is encapsulated with dye/FNP, is suspended in 1 ml pH 2.0 buffer and vortexed for 2 min to ensure complete removal of the model drugs (i.e., dye or FNP) which were encapsulated into MPs with open pores. Then sample was incubated for 2 hrs at 37°C in oven in pH 2.0 buffer to simulate gastric environment. After that, it was centrifuge-washed twice with pH 2.0 buffer at 10,000 rpm for 10 min. Post washing, the pellet was collected and resuspended in 1 ml pH 7.1 solution (described in section 2.4) to open the pores and release model drugs.

2.7 Characterization methods

2.7.1 Scanning Electron Microscopy (SEM)

Field Emission S4800 Electron Microscope (Hitachi, Japan) was utilized to observe the morphology of manufactured MPs, pH responsiveness, and release experiments, and for confirming the closing and opening of MPs. In a typical procedure, MPs suspension was placed on a glass coverslip which was fixed to a double sided carbon tape attached to an aluminum stub, and dried overnight at R.T. A 5 nm thick gold layer was deposited on the samples to minimize the charging effect prior to observation at 15 kV (10 μA).

2.7.2 Dynamic Light Scattering (DLS)

Zetasizer Nano ZS (Malvern Instruments USA, Westborough, MA) was used to measure the size of MPs. DLS measurements were performed with the scattering angle at 173 degree and at 37°C (unless otherwise specified) and with attenuation range from 6 to 9. Refractive index for the polymer was taken from the vendor's data sheet[47].

2.7.3 Fluorescence Microplate reader

Fluorescence of released model drugs (dye and FNP), originally encapsulated into MPs, were measured on a Flexstation® 3 benchtop multi-mode microplate reader ((Molecular Devices, Sunnyvale, California, USA). Fluorescence spectra were monitored at the excitation of 490 nm and emission range of 500-530 nm, with a 1 nm step size. For FNP experiments, excitation wavelength and emission range were fixed at 540 nm and 565-595 nm, respectively. All the measurements were made in Corning 96 wells clear bottom plate with 200 µl sample volume in individual well. Cover tape was used between each experiments to minimize the evaporation of sample that takes place due to long incubation time.

2.7.4 Fluorescence microscope

Fluorescence microscopy analysis was performed using an Olympus IX81 inverted microscope (Olympus, Germany) coupled with DP 80 digital camera having dual CCD sensors. CellSens software (Olympus, Germany) was employed to obtain micrographs captured at 40X objective (Olympus LCPlanFl, 1 µm depth of field, NA 0.6). Samples were placed on a glass slide and imaged after covering with a glass cover slip.

2.7.5 Fourier transform infrared (FTIR) spectroscopy

To analyze the residues of PVA and Tween 20 in the MPs, FTS 7000 FTIR spectrometer (Varian Inc., Palo Alto, CA, USA) equipped with deuterated triglycine sulfate (DTGS) detector, was used to measure the absorbance spectra with a spectral resolution of 4 cm^{-1}. Spectra for freeze dried MPs were compared with the individual spectra of PVA, Tween 20 and original polymer (S100).

2.7.6 Nuclear magnetic resonance (NMR) spectroscopy

To confirm the results obtained from FTIR analysis, NMR spectroscopy was performed with Varian Direct Drive VNMRS 600 spectrometer (Agilent Technologies, Santa Clara CA) operating at a magnetic field strength of 14.1 T (600 MHz ^{1}H frequency) using dimethyl sulfoxide-d_6 (DMSO-d_6) solvent. Measurements were acquired at R.T. using a single pulse excitation with a 45^{o} flip angle of 3.6 µs. Acquisition time was maintained at 1.7 s with repetition time one second. S100, PVA and Tween 20 spectra were recorded separately and used as references for comparison with MPs' spectra.

2.7.7 Differential Scanning Calorimetry (DSC)

To observe any changes in the glass transition temperature (T_g) of MPs, DSC measurements were carried out with a Pyris-1 DSC (Perkin-Elmer, Norwalk, CT, USA) at heating rates of 10°C/min and at a scan rate of 1°C/min. The samples were first cooled from R.T. to -150°C, and then heated to 200°C following 1–2 hr of equilibration in the instrument. For comparison purposes, T_g of original polymer powder was measured.

2.8 Statistics

Data were analyzed using student's t-test or analysis of variance (ANOVA) in Minitab software (State College, PA, USA). A P-value of less than 0.05 indicated a significant difference.

3 Results and Discussion

3.1 Development of pored MPs and study of their pH responsiveness

Very limited research has been reported on fabricating MPs with macropores. Im et al. proposed a method of making pored MPs by freeze-drying a frozen emulsion. This approach has been successful for polystyrene in chloroform solvent[48]. Controlling the rate of solvent evaporation while keeping the solvent below 0°C has been identified as the key reason for pore formation. However, after initial adoption, it has been realized that the approach cannot be widely employed to fabricate pored MPs other than very limited materials such as polystyrene and PMMA. Important to note is that S100 used in this work requires the use of co-solvent mixtures [dichloromethane (T_m: -96.7°C, T_b: 39.6°C), ethanol (T_m: 114°C, T_b: 78.4°C), isopropanol (T_m: -89°C, T_b: 82.5°C); where T_m- melting point, and T_b- boiling point] for dissolution, which caused difficulty in controlling the evaporation rate, a parameter critical to the formation of MPs. As a result, the complicated polymer structure and co-solvent system related to this work rendered previously reported MP formation method futile.

To this end, considering the properties of polymer and solvents involved, a novel and simple method was developed to fabricate MPs with macropores (Figure 3.1). This approach utilizes the classical O/W emulsion technique using a sonicator to form MPs. The evaporation of solvent during sonication induced formation of pores in the MPs at ambient conditions without using freeze drying method. As described in section 2.2.1, after the fabrication of MPs, the emulsion is washed by centrifuge to remove the unwanted solvents, emulsifiers, and detergent. Lastly, the MPs suspension is subjected to rotary evaporation to remove any remaining solvent. Removal of remaining solvent is extremely critical as the MPs are being prepared for vaccine encapsulation and clinical application and any contact with organic solvent might reduce their activity and increase safety concern. Before use, MP sample was filtered to control size to be less than 20 μm, a favorable size range for their enhanced uptake by intestinal cells.

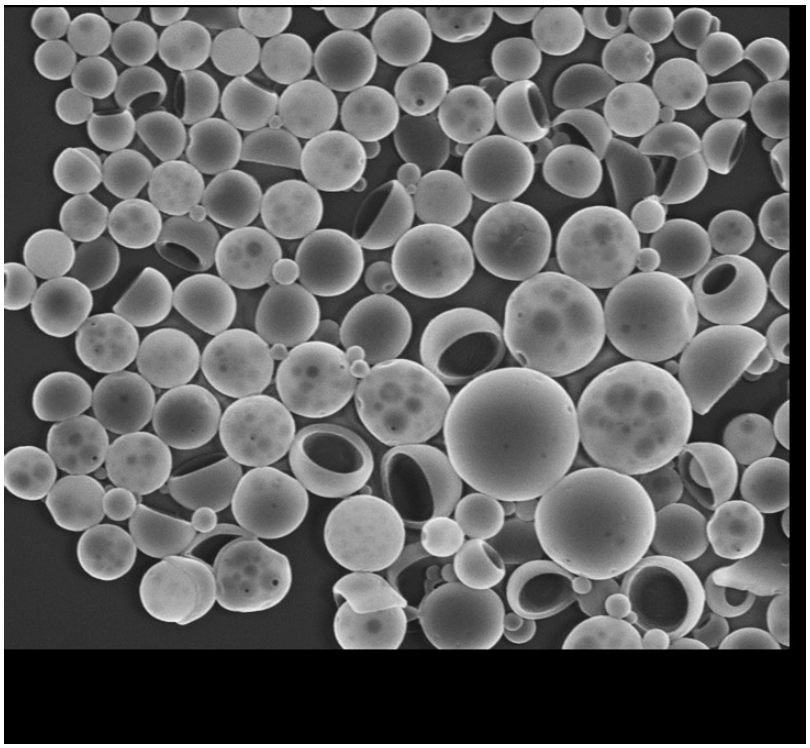

Figure 3.1 SEM images of MPs with macropores. Pored MPs were successfully fabricated using pH sensitive polymer, Eudragit® S100 by a newly developed method

To evaluate the pH responsiveness of MPs in a GI tract environment, MPs were incubated in pH 2.0 buffer as a simulated gastric environment for 2 hrs, and then in pH 7.1 for 4 hrs (average retention time in intestine). Morphological change of MPs at different pH conditions were investigated using SEM analysis. It should be noted that temperature at all testing conditions was controlled at 37°C to mimic physiological environment except a control MP sample in DI water (R.T.). SEM image in Figure 3.2 (a) shows that MPs in DI water maintained their spherical morphology. When exposed to acidic environment (pH 2.0), the size of the MPs

appeared increased compared to the MP suspension at R.T. (compare Figure 3.2 (a) with (b)). However, upon exposure to neutral pH (pH 7.1), a significant morphological change was observed from pored MPs as a result of their dissolution, as shown in SEM image of Figure 3.2 (c).

To verify the size change of MPs, DLS analysis was performed under the same test conditions as in Figure 3.2. The data shows that the size increase of MPs after exposure to pH 2.0 compared to the R.T. control (control: 737.3±67.3 nm, pH 2.0: 930.1±83.7 nm) is attributed to the temperature effect due to no significant difference in the size of MPs between R.T. and 37°C (*t*-test, P = 0.114; DI water: 874.2±67.0 nm, pH 2.0: 930.1±83.7 nm) (see Figure 3.3 (a) for DLS spectra and 3.3(b) for their relative size change). Thus, it is reasonable to assume that acidic environment does not have significant effect on MP properties. As predicted in Figure 3.2 (c), MPs exhibited a bimodal size distribution along with a significant size decrease upon exposure to pH 7.1 (Peak 1: 91.8±11.5 nm, Peak 2: 236.0±42.0 nm). This pH response is consistent with our prediction on the pH response of MPs considering reported material properties of S100. Therefore, it can be concluded that the MPs made of S100 maintains their intact structure in acidic gastric environment, but dissolves in neutral intestinal environment.

a)

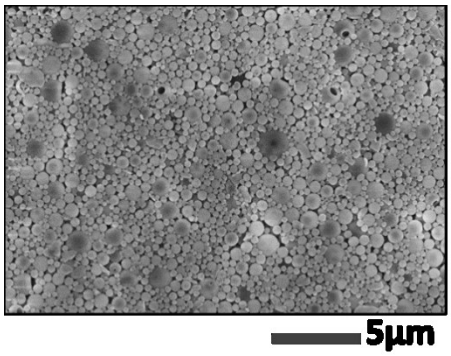

b)

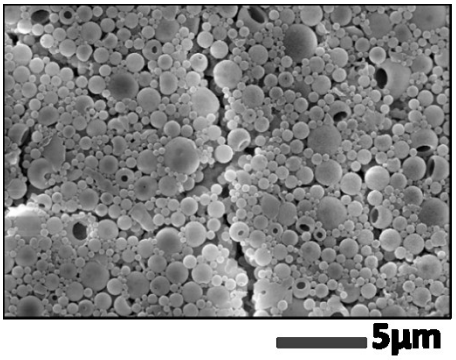

c)

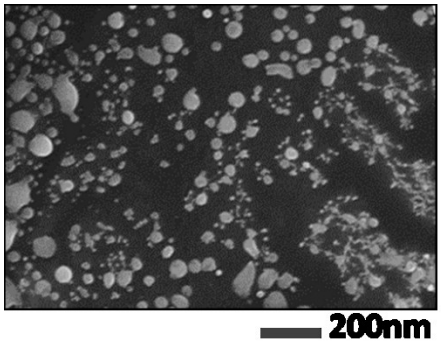

Figure 3.2 SEM images of MPs after being subjected to simulated GI tract pH- a) with no pH/temperature effects (control), b) after 2 hr incubation at pH 2.0 and 37°C, c) after 4 hr incubation of the (b) sample at pH 7.1 and 37°C

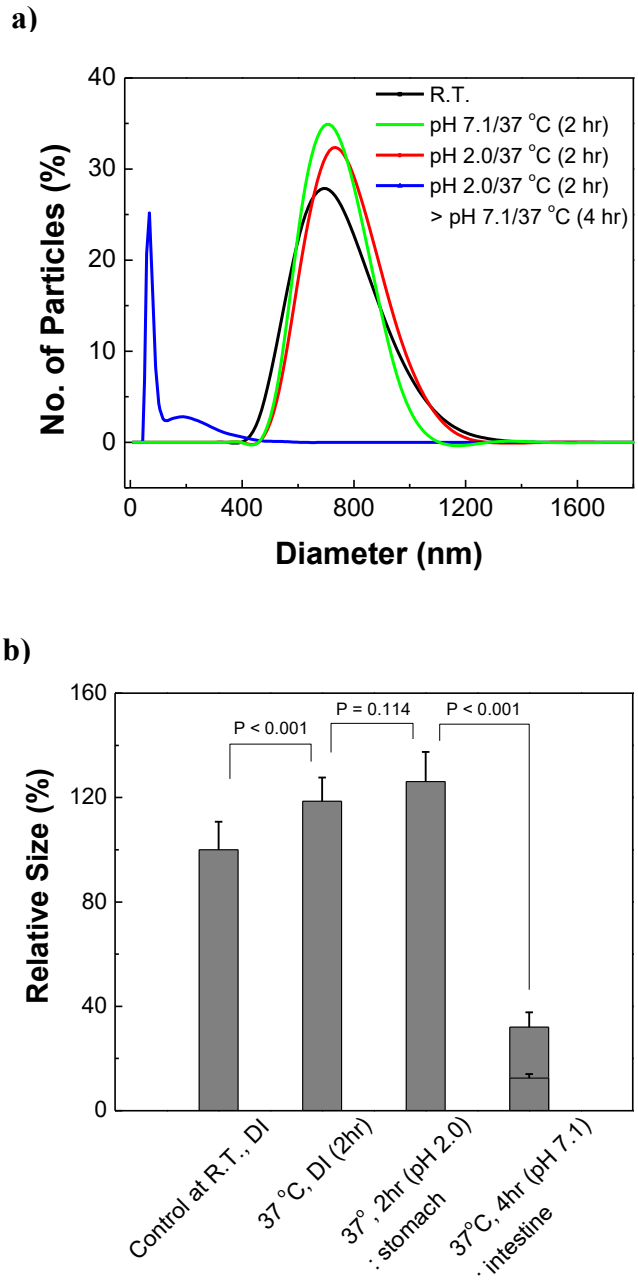

Figure 3.3 Size profile of MPs. (a) DLS spectra of MPs (control in DI at R.T., MPs incubated at pH 7.1/37°C for 2 hrs, MPs incubated at pH 2.0/37°C for 2 hrs, and MPs incubated at pH 7.1/37°C for 4 hrs after 2 hr incubation at pH 2.0) and (b) histogram showing relative size change of MPs

3.2 Effect of process parameters on MP properties

3.2.1 Effect of sonication on emulsion temperature and stability

After the successful fabrication of pored MPs, the next challenge was to optimize process parameters to better control the size of MPs and their pores. To achieve this goal, emulsion forming conditions and evaporation conditions of co-solvent system were varied to obtain optimally functioning pH-responsive MPs with macropores. Since microemulsion technology is being used for making MPs, a great deal of attention was paid to the quality of emulsion for manufacturing MPs. In this work, sonicator has been used to make homogenous emulsion in an efficient way. The major factors deciding the quality of emulsion are sonication time, temperature of the sample due to generation of heat via sonication process, polymer concentration, and sample volume. However, the generation of heat via sonication process should be taken into consideration for better quality of MPs because pore formation of MPs strongly depends on the evaporation rate of organic solvents. Especially, co-solvent system (Dichloromethane: Ethanol: Isopropanol=2:1:1) used in this work to make organic phase in the O/W emulsion is mainly composed of dichloromethane which has relatively low boiling temperature (T_b: 39.6°C).

Keeping the hypothesis that evaporation rate of dichloromethane directly affects the size of pores, time-dependent temperature profiles of three different volumes of

emulsion (50, 100, and 200 ml) were monitored over increasing sonication times (5, 10, 15, 30, and 60 min). The temperature of the room-temperature sonicated 50 ml-sample rose close to 60°C within 10 min, making it extremely difficult to control to evaporation rate of solvents (Figure 3.4 (a)). In the case of 200 ml sample volume, although the sample temperature rose in a controlled manner, the large volume made it difficult to form stable emulsion for different sonication conditions. On the other hand, for the 100 ml sample, the sample temperature rose close to boiling point of dichloromethane in 5 min, followed by a gradual increase up to 64°C in a controlled manner with the increase of sonication time. In addition, 100 ml sample size made the most stable microemulsion under our sonication conditions.

The effects of controlled sonication environment on sample temperature were studied to test potential controllability of sample temperature during sonication. For this purpose, sample container was placed in iced water and the emulsion was prepared by sonication. As shown in Figure 3.4 (b), sonication in iced water exhibited a slow increase in sample temperature over the increase of sonication time. It is also noted that unrefrigerated samples reached T_b (dichloromethane) earlier with increasing sonication time. On the contrary to room-temperature sonication, sonication in iced water did not show any significant temperature increase (Fig. 3.4 (b)). The cooling of the sample container would reduce the temperature rise that is caused by heat generated by sonication. As a result, for all

the different sample volumes, the temperature was always kept below the boiling point of dichloromethane. Since rapid evaporation would make it difficult to control the size of MP pores, cooling the sample by iced water would provide better control on the evaporation rate of solvent. These experiments provided the fundamental understanding of the evaporation rate of solvent during the MPs fabrication process, and later were used as the baseline for designing the experiments for quality control over MPs and their pores sizes.

a)

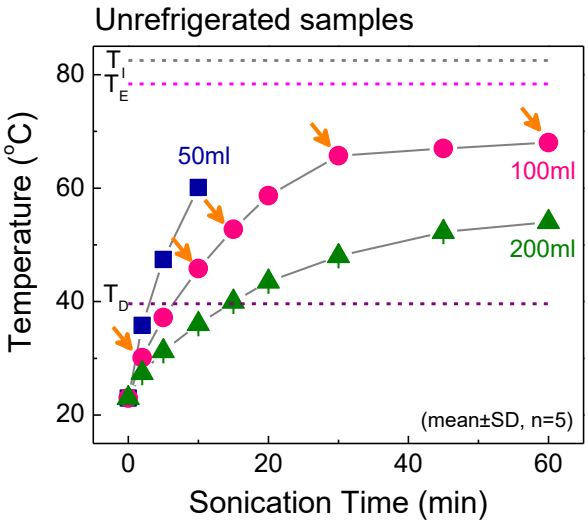

b)

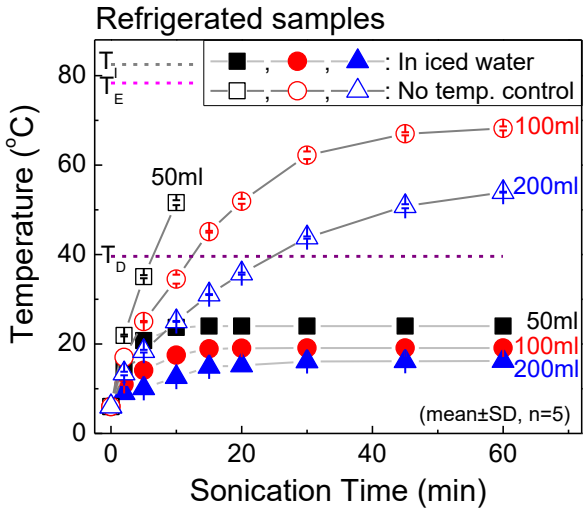

Figure 3.4 Temperature profiles of samples prepared with different sonication conditions at different sample temperature controls- a) unrefrigerated samples (no temperature control), b) refrigerated samples (temperature of sample being controlled by iced water)

3.2.2 Effect of different sonication conditions on MPs

To study the effects of sonication conditions on MP morphology, SEM analysis was performed for both non-controlled (R.T. sonication) and controlled environment (iced water sonication) samples (see Figure 3.5 and 3.6 for R.T. and iced water sonicated samples, respectively). Samples were sonicated at three different time intervals (5 min, 30 min, and 60 min) for two different sonication methods (i: discontinuous sonication and ii: continuous sonication), as described in section 2.2.2. Figure 3.5 shows representative SEM images of MPs prepared by R.T. sonication. As shown in Figure 3.5, the continuous sonication generated MPs with heterogeneous pore sizes. On the other hand, as expected, control over the population of the big pores in discontinuous sonication was relatively better probably due to slow solvent evaporation. Also, even the smaller particles were found to have pores unlike the continuous samples, where only the bigger particles formed pores. Therefore, although the MPs prepared by R.T. sonication maintained their spherical morphology, less control was observed in terms of the pore formation. In contrast, MPs prepared by iced water sonication did not generate spherical morphology for discontinuously sonicated samples (Figure 3.6 i), but for continuous sonication, it required more than 30 min to form MPs with spherical morphology (Figure 3.6 ii). Moreover, iced water sonicated MPs appeared to form smaller pores in comparison of R.T. sonicated MPs, which can be explained by

slower solvent evaporation rate. Therefore, these results supported the possibility of controlling the pore size of MPs by sample temperature, and the importance of slow solvent evaporation.

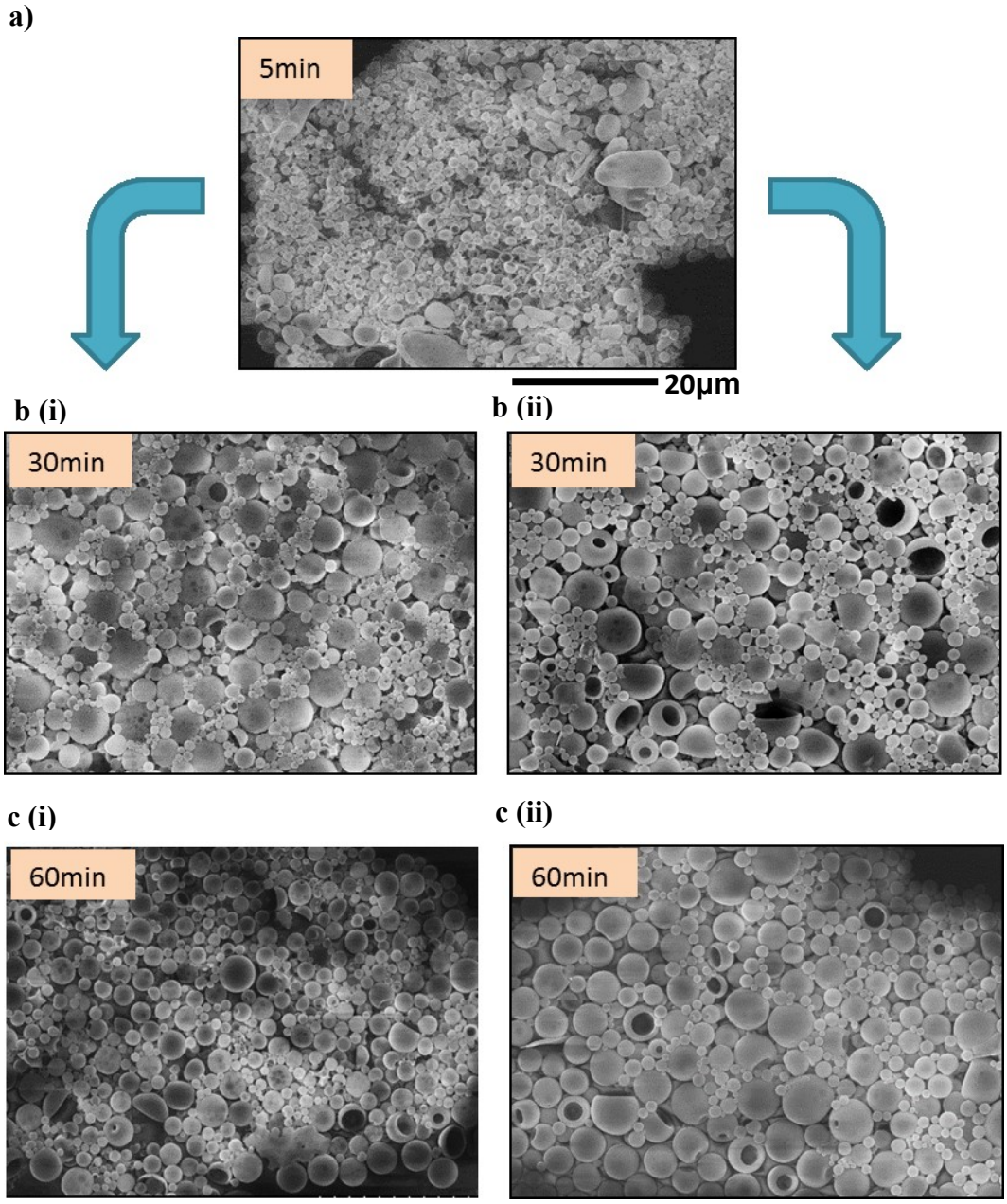

Figure 3.5 SEM images of MPs prepared by room temperature R.T. sonication for different sonication conditions deployed for different time intervals a) 5 min continuous sonication, b) i, 30 min discontinuous sonication, b) ii, 30 min continuous sonication, c) i, 60 min discontinuous sonication, and c) ii, 60 min continuous sonication

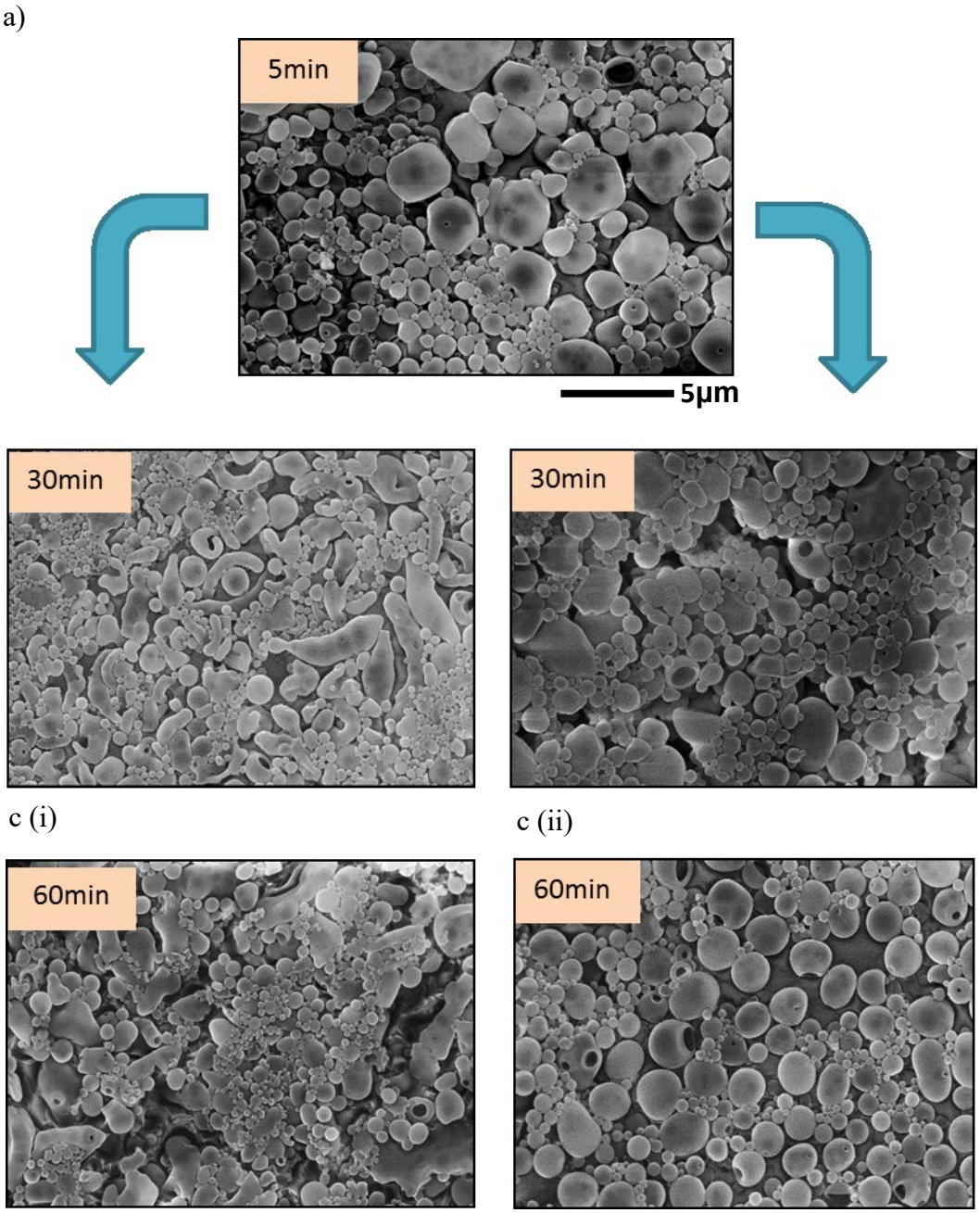

Figure 3.6 SEM images of MPs prepared in iced water sonication (sample temperature controlled by iced water surrounding it) for different sonication conditions deployed for different time intervals a) 5 min continuous sonication, b) i, 30 min discontinuous sonication, b) ii, 30 min continuous sonication, c) i, 60 min discontinuous sonication, c) ii, 60 min continuous sonication

3.2.3 Effect of slow solvent evaporation on MPs

To maximize the advantages of slow solvent evaporation, we proposed an idea of sonication, followed by magnetic stirring for emulsions. It is hypothesized that initial sonication process should be able to make stable emulsion at < 39.6°C and the level of evaporation can be simply controlled by adjusting stirring time. For this purpose, MPs were prepared by 5 min sonication both at R.T. and in iced water (IW). Post sonication process, O/W emulsion was magnetically stir incubated at R.T. (at 700 rpm) for various time intervals (0, 2, 4, and 8 hrs) (see section 2.2.3 for detailed conditions). SEM data in Figure 3.7 show that enough incubation of sonicated emulsion is important parameter to make spherical particles. Sonicated emulsion without incubation resulted in the formation of non-spherical morphology, however evolved into spherical shape with the increase of incubation time. In addition, longer incubation had a tendency to form bigger pores. Similarly, IW incubated samples exhibited non-spherical morphology and further incubation had an increase in the population of spherical MPs as shown in Figure 3.8. Thus, it is assumed that incubation time plays a critical role in determining emulsion stability, morphology of MPs, and size of pores. It is important to remember that while MP morphology deviates from the sphere, as far as non-spherical particles have pores, they can still be used for encapsulating drugs.

MP samples were further characterized by DLS analysis to characterize size distribution and polydispersity index (PDI). As shown in Figure 3.9 (a), the particle size did not show significant difference at all the time intervals in both the sample conditions, i.e. R.T. and IW samples. However, completely different pattern of the PDI was observed from R.T. and IW samples. As shown in Figure 3.9 (b), R.T. samples did not exhibit any significant difference in PDI values over the increase of incubation time (ANOVA, $P > 0.1$). On the other hand, the IW sample group exhibited a significant decrease in PDI with increasing incubation time (ANOVA, $P < 0.001$). Although further research is needed to support our observation, it is believed that the difference might be related to the morphological change of the particles as well as temperature-induced aggregation depending on sample preparation conditions.

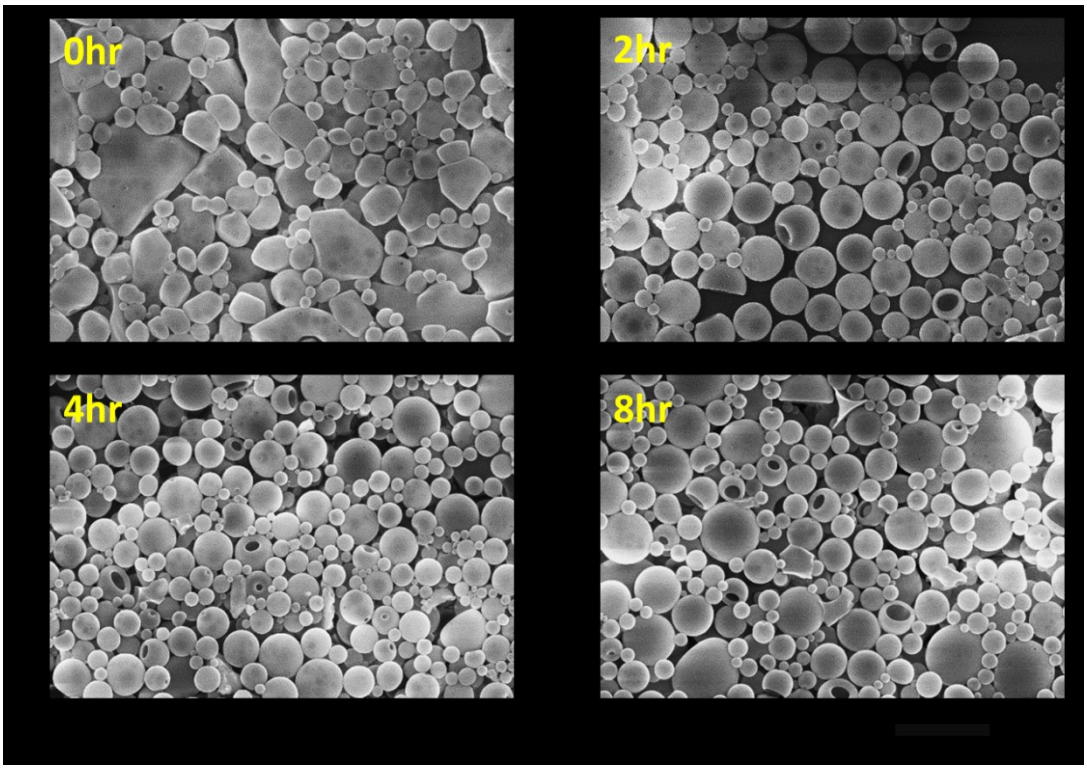

Figure 3.7 SEM images of pored MPs prepared by 5 min R.T. sonication, followed by stir incubated for different time intervals: a) 0 hr, b) 2 hrs, c) 4 hrs, and d) 8 hrs

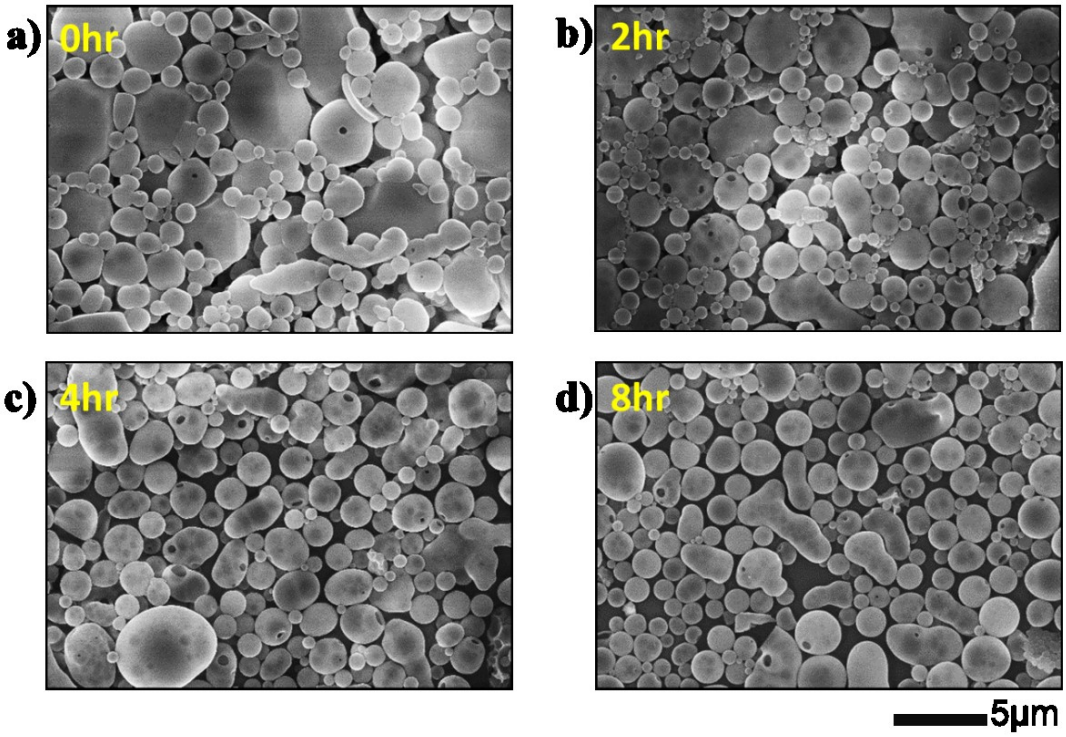

Figure 3.8 SEM images of pored MPs prepared by 5 min iced water sonication, followed by stir incubated for different time intervals: a) 0 hr, b) 2 hrs, c) 4 hrs, and d) 8 hrs

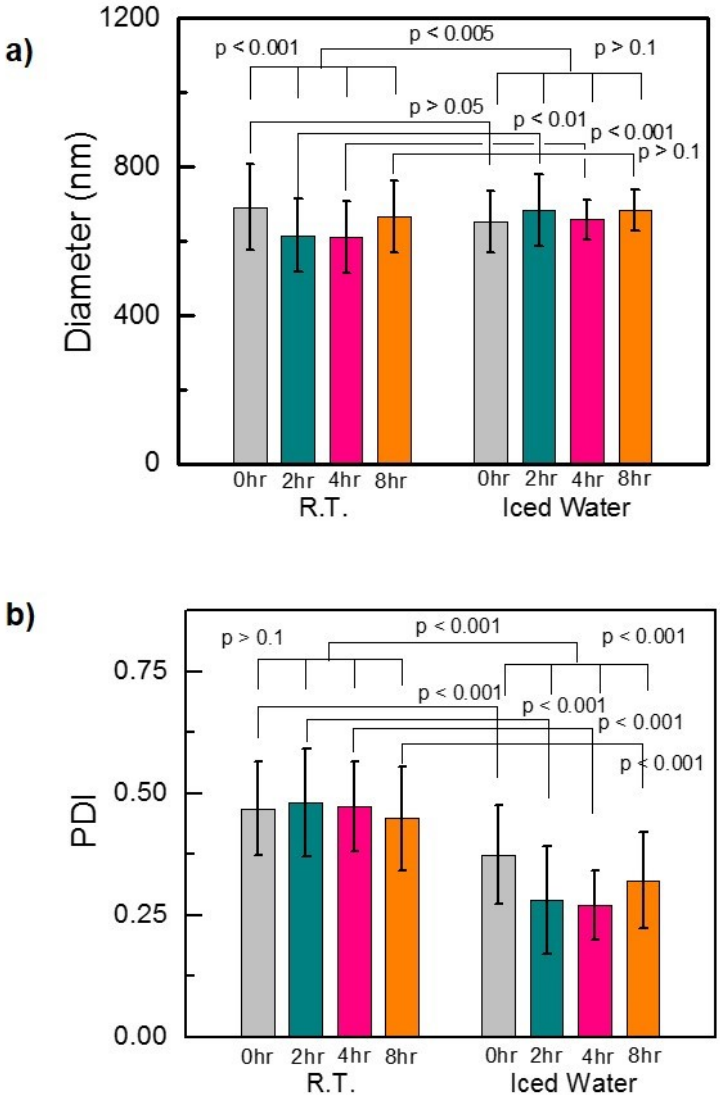

Figure 3.9 a) Size and b) polydispersity index (PDI) profiles of MPs prepared at R.T. and IW conditions with application of sonicator for 5 min followed by magnetically stirred for different time intervals

3.2.4 Study of pore size distribution of MPs

To further evaluate the effects of sample preparation conditions on the pore size of MPs, the relative size of pores and MPs was determined by analyzing SEM images (representative images were selectively shown in Figures 3.7 and 3.8). The data shows that the relative pore size of R.T. sonicated MPs tends to increase with incubation time in contrast to no significant change for iced water sonicated MPs (R.T. MPs: ANOVA, $P < 0.001$, iced water MPs: ANOVA, $P > 0.05$; see histogram of R.T., Figure 3.10 (a), and iced water samples, Figure 3.10 (b), and (c) for analysis plots). This difference in pore size change can be explained by the different sample temperatures. That is, initial high temperature coupled with incubation at R.T. account for higher evaporation of solvents, leading to the formation of time-dependent pore size increase. In contrast to R.T. incubation, low sample temperature of IW incubation samples can suppress temperature increase and slow the evaporation of solvents. This explains why no significant level of pore size increase was not observed from IW samples.

Based on the above results, three MP fabrication conditions (i.e., 30-10-30, R.T., and IW) are suggested for further encapsulation tests (see section 2.2.4 for detailed conditions). It should be noted that 30-10-30 formed MPs with biggest pores amongst all three conditions due to the high evaporation rate of solvents due to longer sonication period. R.T. and IW incubation samples were selected due to the

advantages of simple fabrication process compared to 30-10-30 conditions, and large pore formation and high MP yield, respectively.

a)

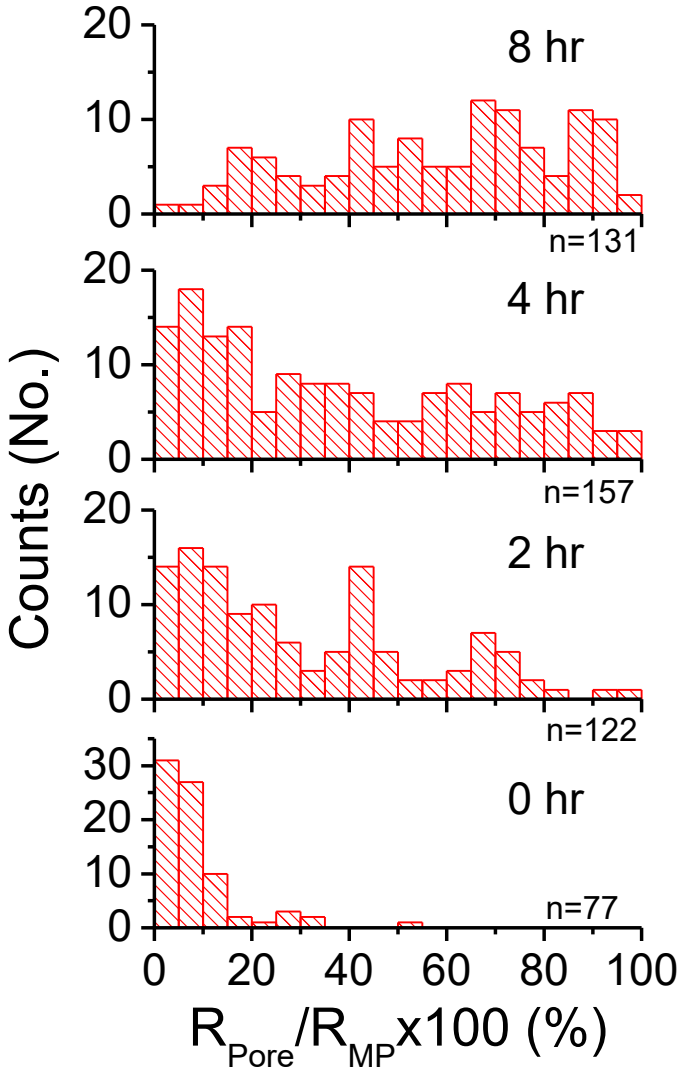

Figure 3.10 a) Histogram of MPs to pore size ratio for MPs prepared at R.T condition with magnetically stirred for different time intervals

b)

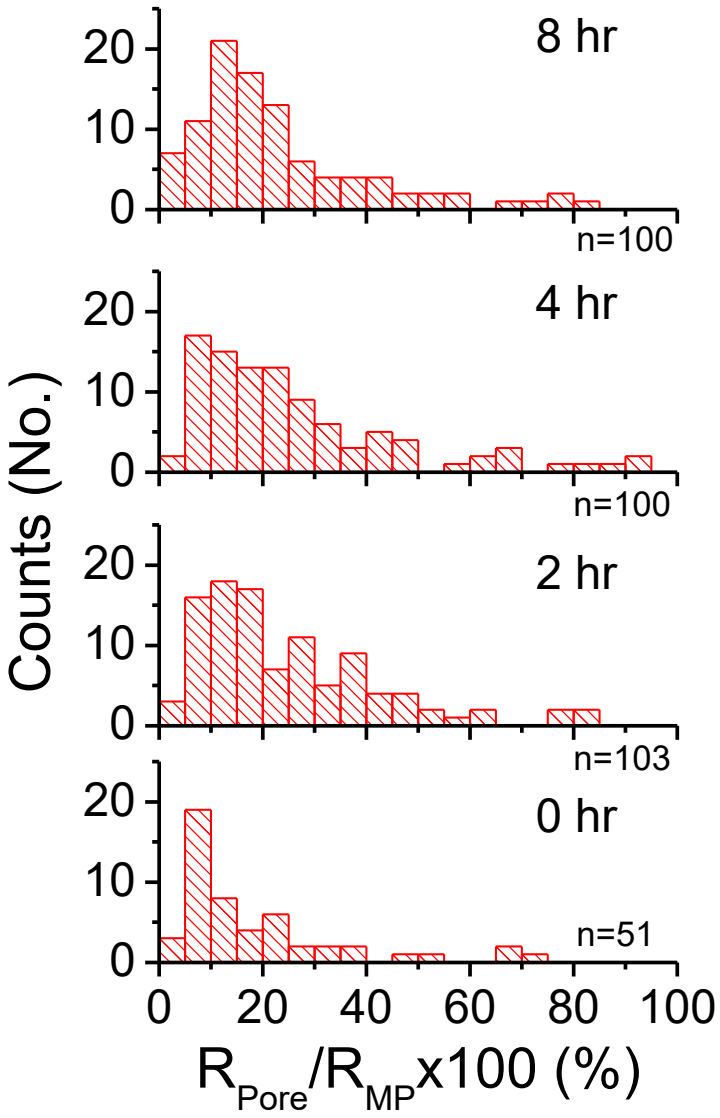

Figure 3.10 b) Histogram of MPs to pore size ratio for MPs prepared at IW condition with magnetically stirred for different incubation time intervals

c)

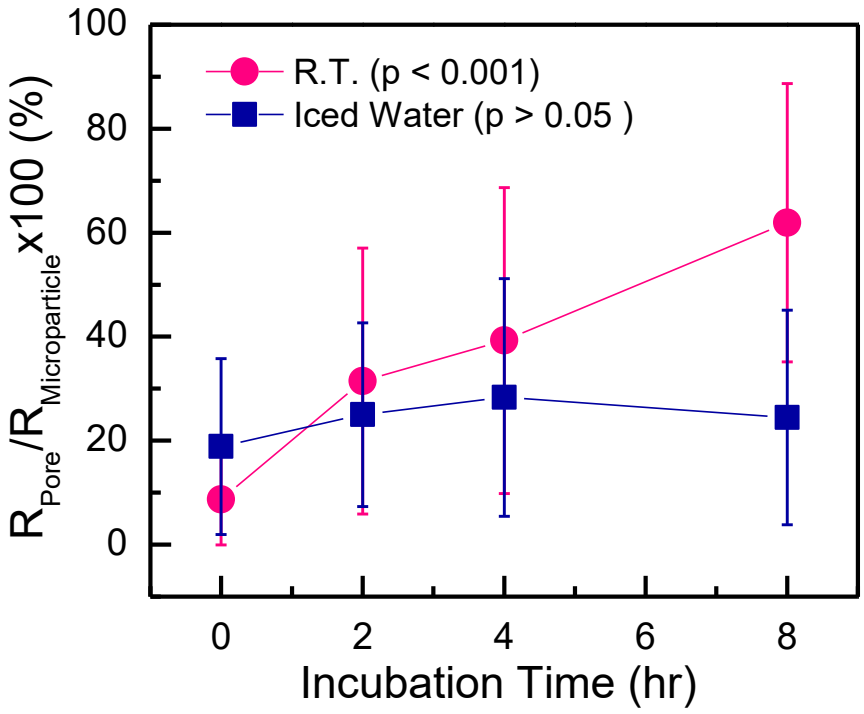

Figure 3.10 c) Profile of MPs to pore size ratio for MPs prepared at R.T. and IW conditions with magnetically stirred for different incubation time intervals

3.3 Viability of pored MPs for model drugs encapsulation

In order to confirm the hollow structure of MPs as predicted from the SEM images in the previous section, and also to test potential applicability of pored MPs for various drugs encapsulation, sulforhodamine b (abbreviated as SB) was encapsulated as a model drug into R.T. and IW incubation samples. Fluorescence microscopy images in Figures 3.11 and 3.12 clearly demonstrate that SB was encapsulated inside MP pores in comparison with control images. Specifically, first control sample in the experiment was only MPs, which did not fluoresce (see Figure 3.11 (a) for R.T. incubation sample and Figure 3.12 (a) for IW incubation sample). Next, as a second control, MPs and drugs were mixed together, which also did not generate significant level of fluorescence from MPs as can been seen from fluorescence images of Figure 3.11 (b) and Figure 3.12 (b) for R.T. and IW incubation samples, respectively. It is evident that only SB encapsulated MPs generated highest level of fluorescence intensity, shown in Figure 3.11 (c) for R.T. incubation sample and Figure 3.12 (c) for IW incubation sample, confirming the successful encapsulation of dye inside the pore of MPs.

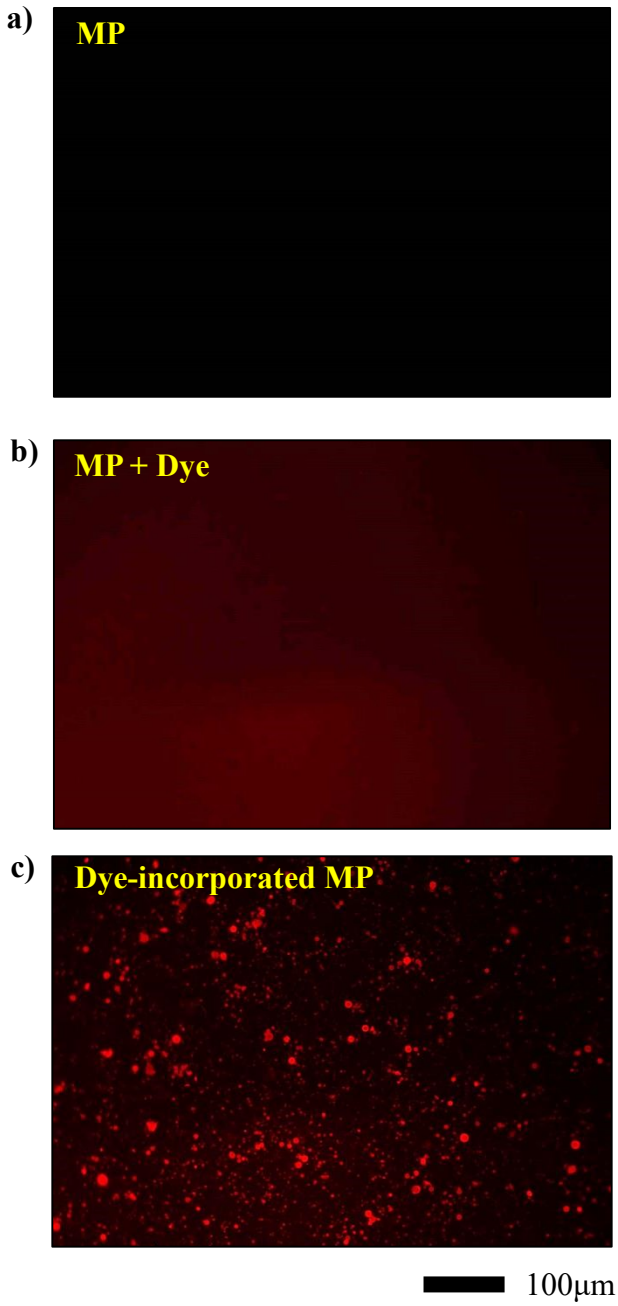

Figure 3.11 Fluorescence micrographs of a) MPs only, b) MPs and sulforhodamine b (SB) dye mixture, c) SB encapsulated MPs. MPs were prepared using R.T. incubation condition with 4 hr magnetic stir incubation.

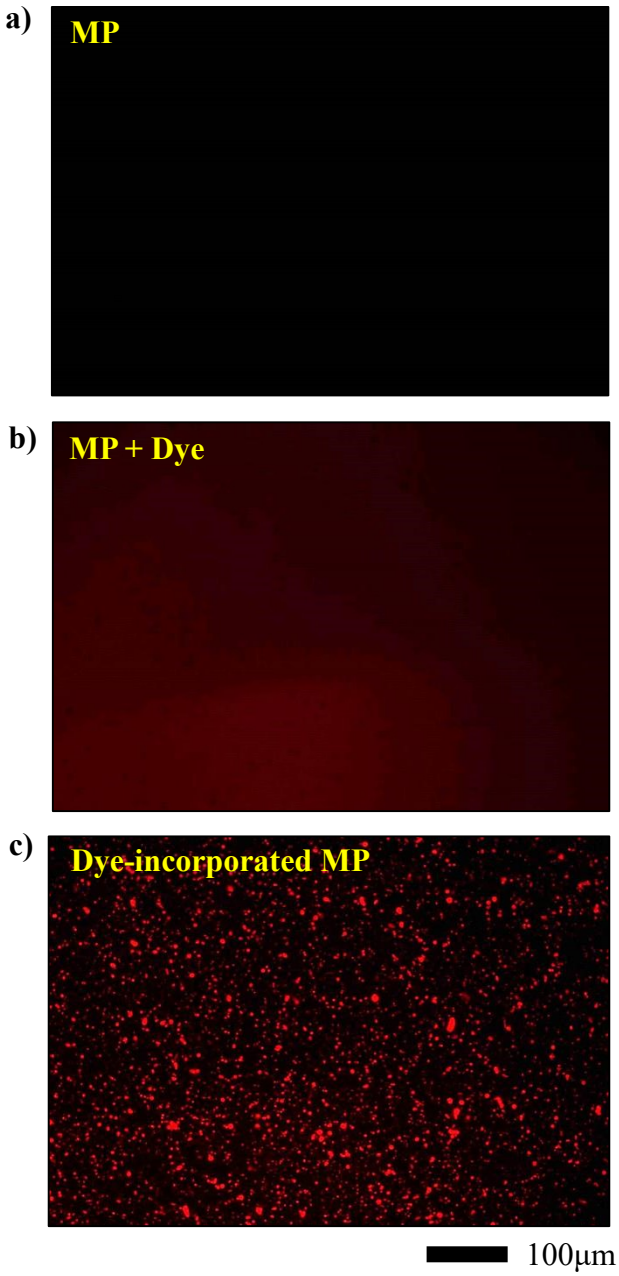

Figure 3.12 Fluorescence micrographs of a) MPs only, b) MPs and sulforhodamine b (SB) dye mixture, and c) SB encapsulated MPs. MPs were prepared using IW incubation condition with 4hr magnetic stir incubation.

3.4 Development of a novel method to close the pores of MPs

At the beginning of this work, the research approach was to prepare pored MPs from pH sensitive polymer, which would close the pores at acidic pH of stomach in order to protect the encapsulated vaccine from gastric juice, and would later open the pores or dissolve in the neutral environment of intestine to release the vaccine. To meet the goal, one of the most significant technical challenges was to develop a method to completely close pores of vaccine-encapsulated MPs. Furthermore, the pore sealing method must be compatible with existing pharmaceutical fabrication process and biopharmaceuticals (i.e. vaccine) to maintain their efficacy.

Hence, a first-of-its-kind method based on freeze drying was developed to close the pores of MPs (see section 2.3 for detailed process conditions). Our newly developed pore closing method completely sealed the pore of original MPs as analyzed by SEM (see Figure 3.13 (a) for the original pored MPs and Figure 3.13 (b) for MPs after the application of freeze drying). Another significant finding is that MPs with sealed pores reopened their pores upon exposure to water as shown in Figure 3.13 (c). The significance of our experimental results lies in the demonstration of the feasibility of our proof-of-concept pH-responsive MP vaccine delivery system.

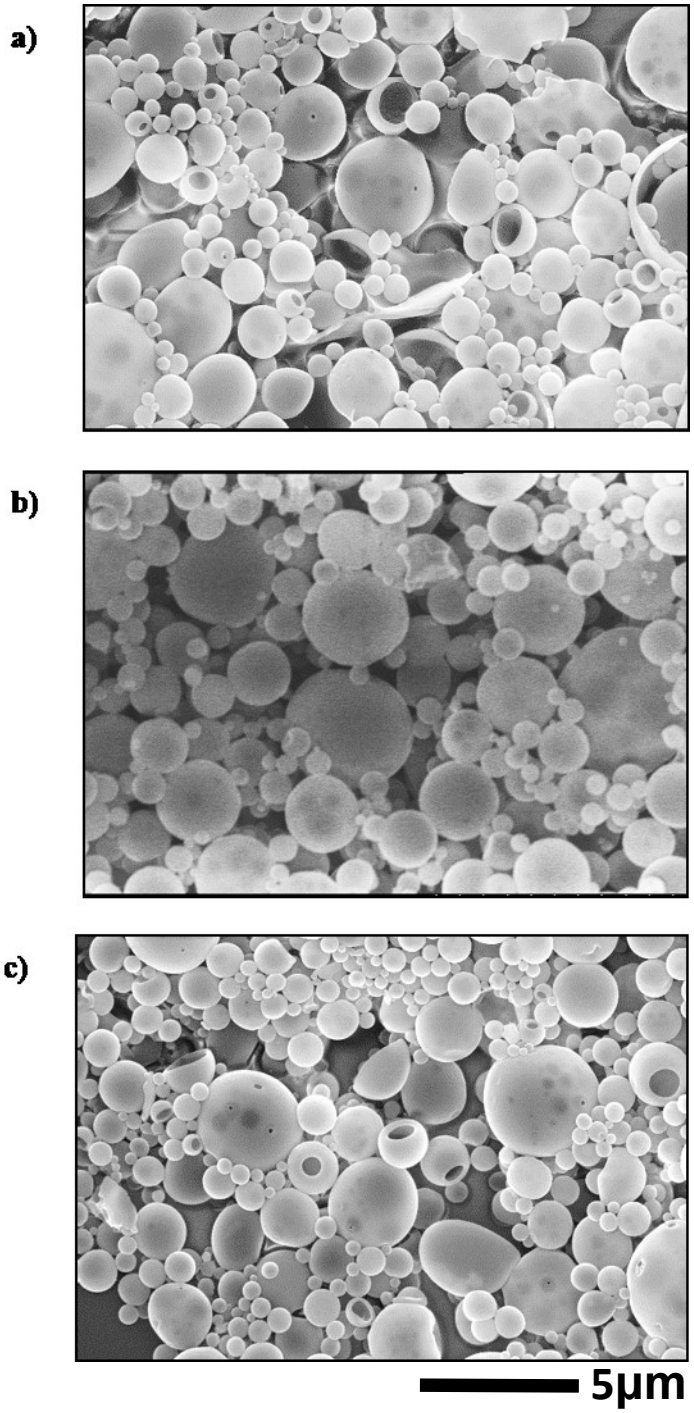

Figure 3.13 SEM images of micro-particles a) original b) after pore closure, and c) after re-opening of pores

The next challenge was to understand the reason behind the pore closure post freeze drying process. The initial theory proposed was that the pores were sealed due to intra-mass transfer in polymeric MPs as a result of lowered glass transition temperature of the polymer comprising MPs. As a first step, we performed DSC analysis to measure T_g of MPs and found that MPs exhibited significant decrease in T_g compared to that of original polymers as can be seen in Figure 3.14.

Next, we performed FTIR analysis to investigate the incorporation of PVA or Tween 20 into MPs. Since PVA and Tween 20 are being used in preparation of MPs, their incorporation into MPs might lower T_g due to plasticizing effect of Tween 20 and lower T_g of PVA compared to S100 polymer (T_g of S100: > 135°C, T_g of PVA: ~85°C)[49,50]. As shown in Figure 3.15, FTIR spectra of MPs (30-10-30, R.T., and IW) exhibited bands at 2860 cm^{-1} and 2920 cm^{-1}, which is consistent with characteristic peaks of Tween 20 and Tween 20/PVA, respectively. The presence of characteristic Tween 20 peak on MPs at 2860 cm^{-1} indicates that Tween 20 has been incorporated into MPs. However, due to the characteristic peak overlapping at 2920 cm^{-1} for Tween 20 and PVA, ^{1}H-NMR was performed to identify the presence of PVA. From the comparison of ^{1}H-NMR spectra of pored MPs with S100 polymer, Tween 20, and PVA in Deuterated DMSO (Figure 3.16), it was evident that PVA was not incorporated into MPs, but only Tween 20. Therefore, although systematic investigation needs to be further performed, it is presumed that the incorporation of Tween 20 used to make O/W emulsion contributed to the

decrease of T_g of MPs and played a significant role in pore sealing process by facilitating molecular movement.

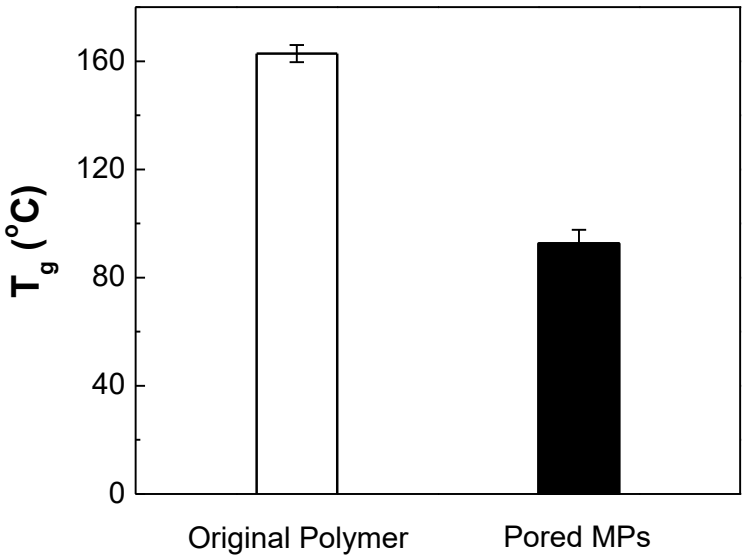

Figure 3.14 DSC spectra of original polymer and pored MPs

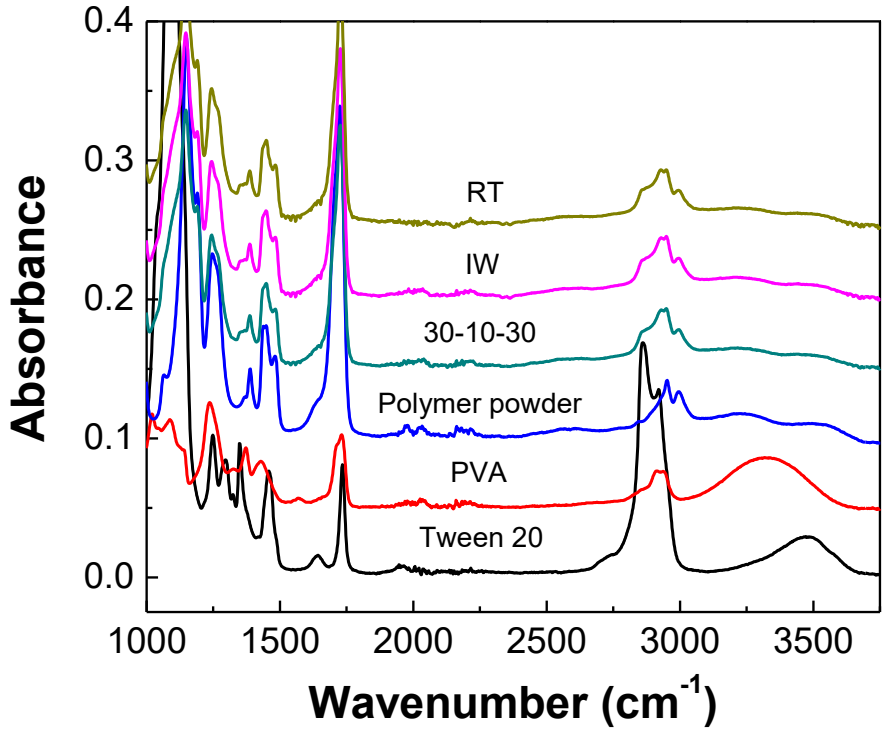

Figure 3.15 FTIR spectra of MPs prepared with different process conditions and of original polymer, PVA, and Tween 20

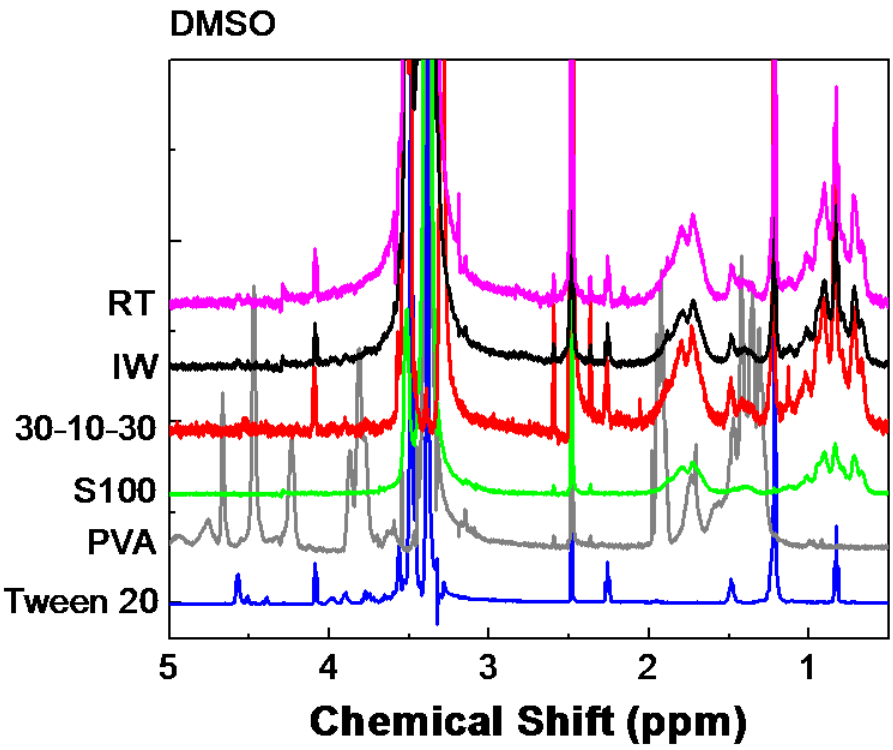

Figure 3.16 ^{1}H NMR analysis of MPs prepared with different process conditions and of original polymer, PVA, and Tween 20

3.5 Time dependent pH responsiveness of pored MPs

After the successful sealing of MP pores, time-dependent pH response of 30-10-30, R.T., and IW MPs were investigated in the simulated GI tract environment. MPs with closed pores were subjected to first, pH 2.0 buffer for 2 hrs to investigate their behavior in stomach environment, and then subsequently subjected to pH 7.1 buffer for 4 hrs to study their behavior in intestine environment. SEM analysis confirmed that the pores of the MPs remain virtually unaffected by the exposure and incubation in pH 2.0 buffer (see Figure 3.17 (b) for 30-10-30, Figure 3.18 (b) for R.T., and Figure 3.19 (b) for IW). Also, when the MPs were subjected to pH 7.1, they either opened the pores or dissolved for all the different condition, as can be seen from the SEM images - 30-10-30 (Figure 3.17 (c)), R.T. (Figure 3.18 (c)), and IW (Figure 3.19 (c)). These results were in coherence with the expected outcome, as the polymer used to prepare MPs, doesn't respond to acidic pH but dissolves in the neutral pH. These findings were extremely critical for the project as they prepared the ground work for further experiments for encapsulating model drugs, which can be protected in gastric environment, and successful released in intestine, to demonstrate the proof-of-concept.

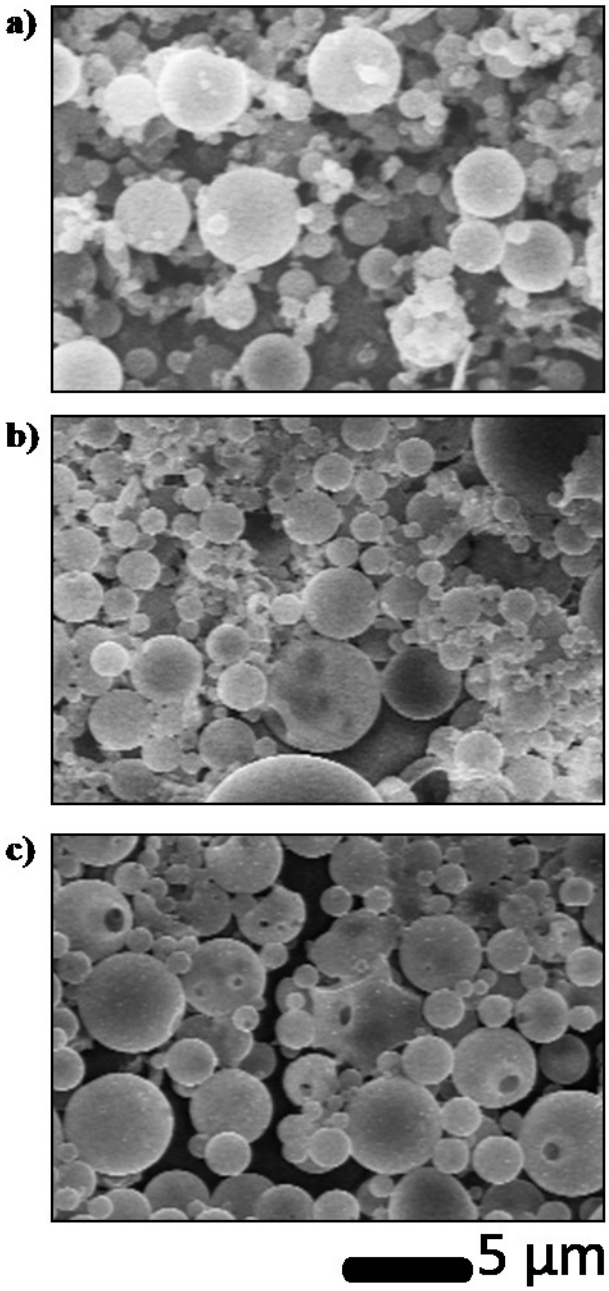

Figure 3.17 SEM images of MPs prepared under 30-10-30 condition, followed by freeze drying to close the pores, and after being subjected to simulated GI tract pH- a) with no pH/temperature effects (control), b) after 2 hr incubation at pH 2.0 and 37°C, c) after 4 hr incubation of the (b) sample at pH 7.1 and 37°C

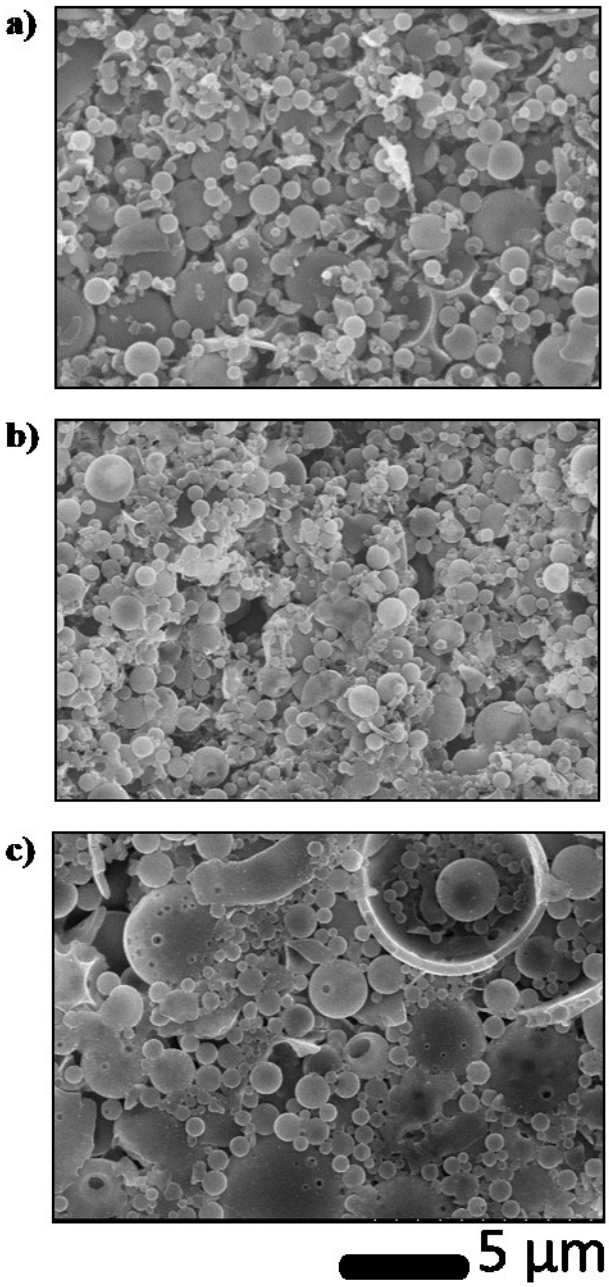

Figure 3.18 SEM images of MPs prepared under R.T. condition, followed by freeze drying to close the pores, and after being subjected to simulated GI tract pH- a) with no pH/temperature effects (control), b) after 2 hr incubation at pH 2.0 and 37°C, c) after 4 hr incubation of the (b) sample at pH 7.1 and 37°C

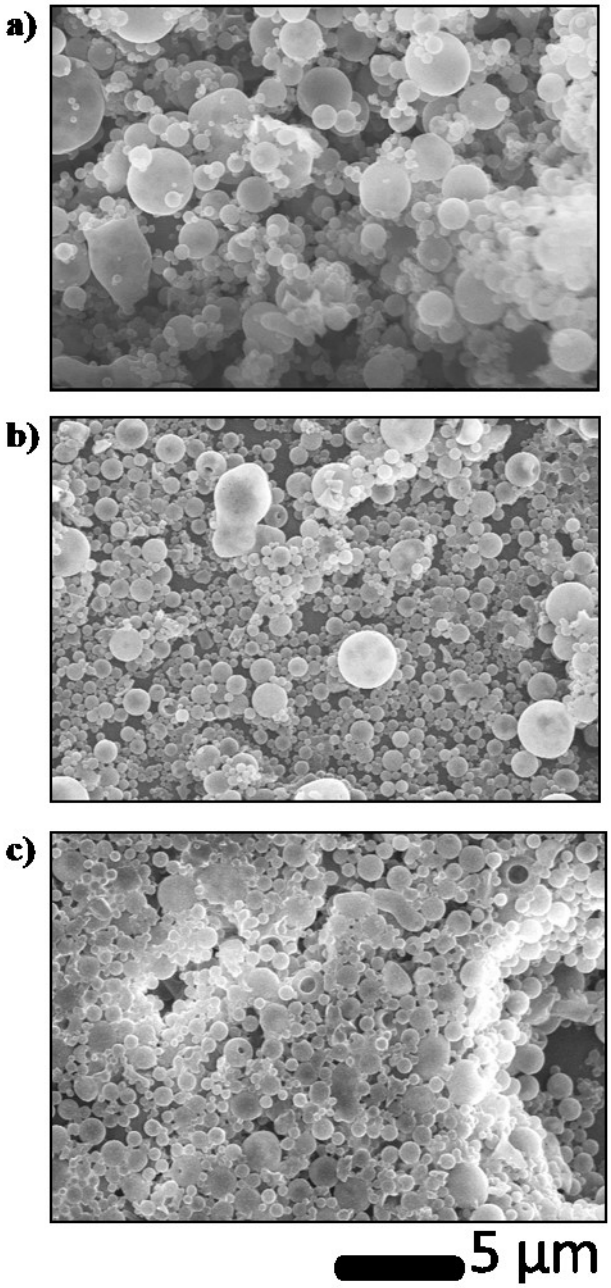

Figure 3.19 SEM images of MPs prepared under IW condition, followed by freeze drying to close the pores, and after being subjected to simulated GI tract pH- a) with no pH/temperature effects (control), b) after 2 hr incubation at pH 2.0 and 37°C, c) after 4 hr incubation of the (b) sample at pH 7.1 and 37°C

3.6 Encapsulation of model drugs and study of their release behavior

To examine the applicability of pored MPs in a GI tract environment, two model drug-encapsulated MPs were prepared following the protocol described in section 2.6, i.e.100 nm FNP and SB. Fluorescence Microscopy (FM) was initially performed only for FNP to observe its encapsulation and pH-dependent release behavior through visual inspection. As can be seen in the Figure 3.20, FNP-encapsulated MPs (FNP-MPs) maintained their intact structure over the course of incubation at pH 2.0 for 2 hrs, thus no significant fluorescence intensity difference was observed from 30-10-30, R.T., and IW samples due to leakage of FNPs. It is interesting to note that when 2 hr incubated FNP-MPs in acidic environment were exposed to pH 7.1, MPs showed a rapid leakage within 20 min and only 100nm-sized FNPs were observed after 4 hr incubation at pH 7.1 (images of 4hr-incubated samples are shown in Figure 3.20). This can be explained by pore opening/dissolution due to pH increase, which is consistent with our prediction. These experiments indicate that the pored MP system can encapsulate model drugs and protect them from the gastric environment, and can release them in intestine environment.

After the qualitative analysis concluded by FM experiments, fluorescence measurements were performed to quantify the time-dependent release of model

drugs in order to get a better picture of pH response. The variation in fluorescence intensity was monitored over the increase of incubation time, i.e. 2 hrs at pH 2.0 and 4 hrs at pH 7.1. As shown in Figures 3.21 (a) and (b), no significant level of fluorescence intensity change was observed during the 2 hr incubation period in pH 2.0. This is attributed to the absence of FNP leakage from MPs. However, exposure to pH 7.1 induced a significant dye release during the initial 20 min, followed by saturation in release profile around 60-65% within an hour. This pH-responsive release behavior of MPs is consistent with our fluorescence microscopy analysis. On the other hand, as shown in Figures 3.22 (a) and (b), SB-MPs (30-10-10 and IW) exhibited a biphasic release behavior: an initial release up to 14-20% at 20 min upon exposure to pH 2.0, followed by a rapid increase up to 85-90% within 10 min. As indicated in the plateau at 20 min, the absence of further fluorescence intensity change indicates that the leak occurring in the beginning of incubation of sample, could be attributed to the leaks of SB from unclosed MPs. When exposed to pH 7.1, a steep increase in release rate was followed by a plateau (85-90%) within 10 min. The more rapid release profile of SB-MPs can be explained by the smaller size of SB compared to FNPs. It is important to note that total release rate is calculated based on the assumption that all SB dyes are encapsulated into closed MPs. Therefore, we expect that characterization of the pore closure efficiency by freeze drying would be important to estimate precise release profile.

These experiments gave an insight into the release profile of MPs encapsulated with model drugs. With no significant leak in acidic pH and a rapid release in neutral pH will enable our drug delivery system to counteract the technical challenges associated with development of oral influenza vaccine.

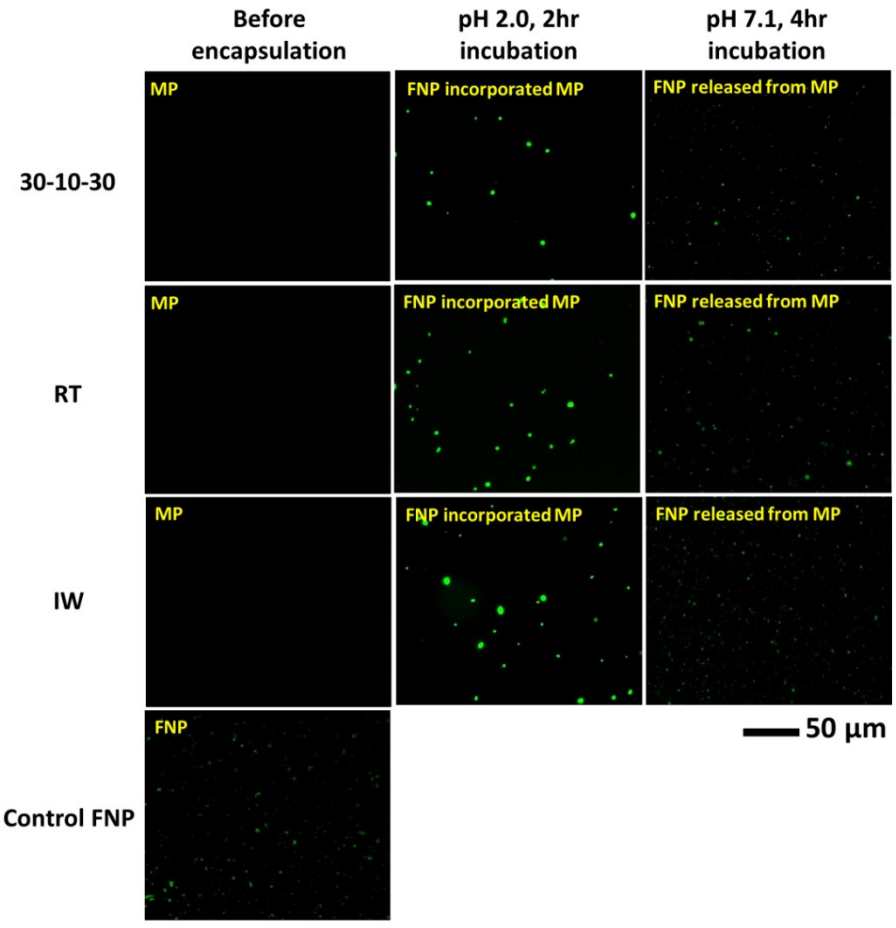

Figure 3.20 Fluorescence micrographs of FNP encapsulated MPs (30-10-30, R.T., and IW) subjected to simulated GI tract environment (stomach: 2 hr incubation at pH 2.0 and 37°C, and intestine: 4 hr incubation at pH 7.1 and 37°C). As a control, fluorescent micrographs of MPs without FNP and FNP are shown for comparison.

a)

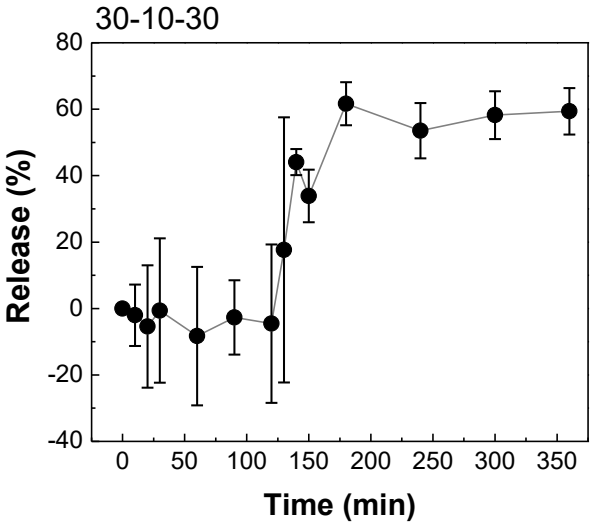

b)

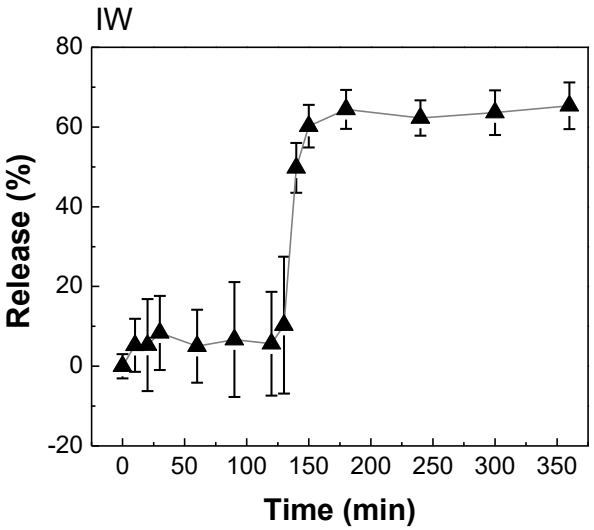

Figure 3.21 Time dependent release profile of encapsulated 100 nm FNPs from MPs prepared at a) 30-10-30, and b) IW conditions and subjected to pH 2.0 for 2 hrs, followed by pH 7.1 for 4 hrs to simulate GI tract

a)

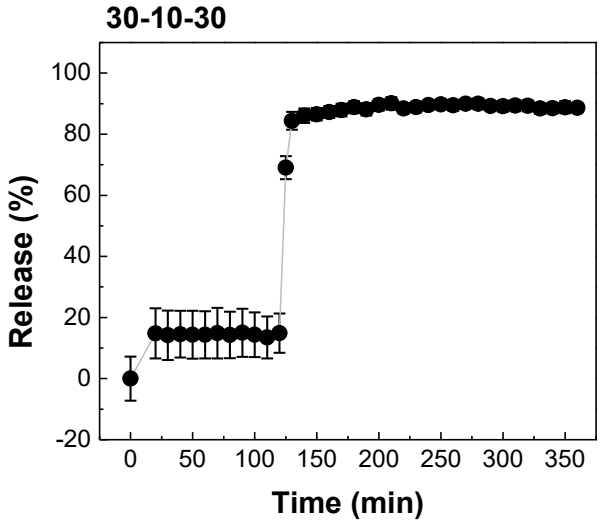

b)

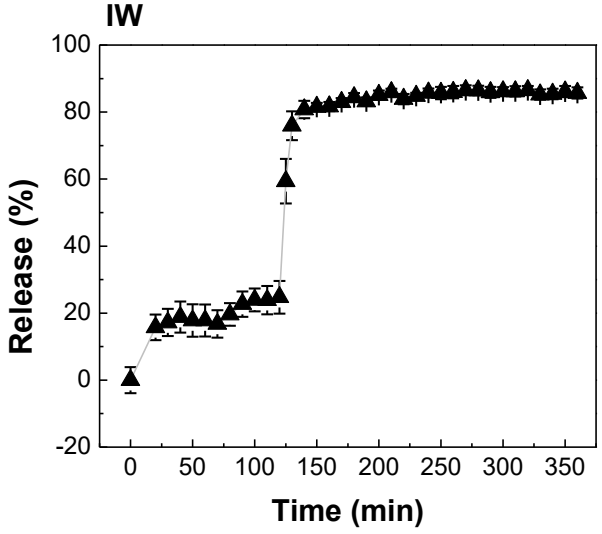

Figure 3.22 Time dependent release profile of encapsulated sulforhodamine b from MPs prepared at a) 30-10-30, and b) IW conditions and subjected to pH 2.0 for 2 hrs, followed by pH 7.1 for 4 hrs to simulate GI tract

3.7 Recyclability of pored MPs

After the proof-of-concept experiments for the encapsulated model drugs, next step was to investigate the recyclability of pored MPs. In case of pored MPs, recyclability can be defined as the ability to obtain the closed pored MPs after freeze drying, reopening the pores and then closing them again, for multiple cycles. Also, the prerequisite for recyclability is that the MPs quality shouldn't deteriorate with passing of each cycle. This quality can be extremely useful in case of encapsulation of complex drugs. Experiments were performed as explained in section 2.5 for testing this behavior. From the SEM images (Figure 3.23 for 30-10-30 and Figure 3.24 for IW), it can be concluded that even after applying 10 freeze drying cycles, MPs maintained their pH responsive properties. These findings will help in designing of complex drug delivery systems.

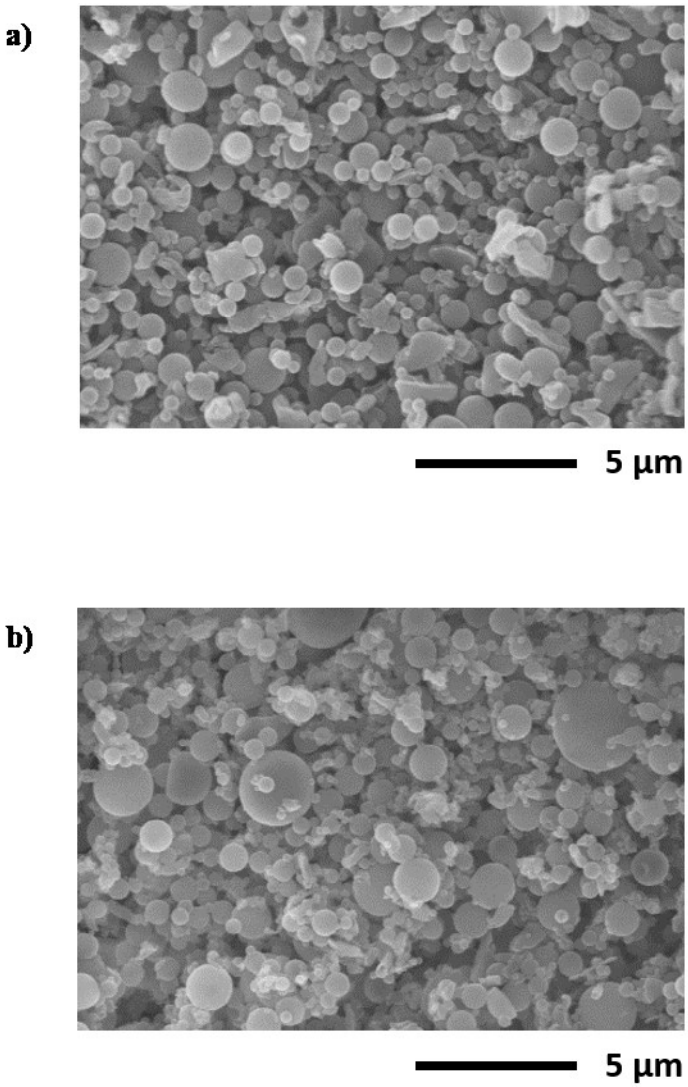

Figure 3.23 SEM images of MPs prepared at 30-10-30 condition and subjected to multiple freeze drying cycles- a) after first freeze dry cycle and b) after tenth freeze dry cycle

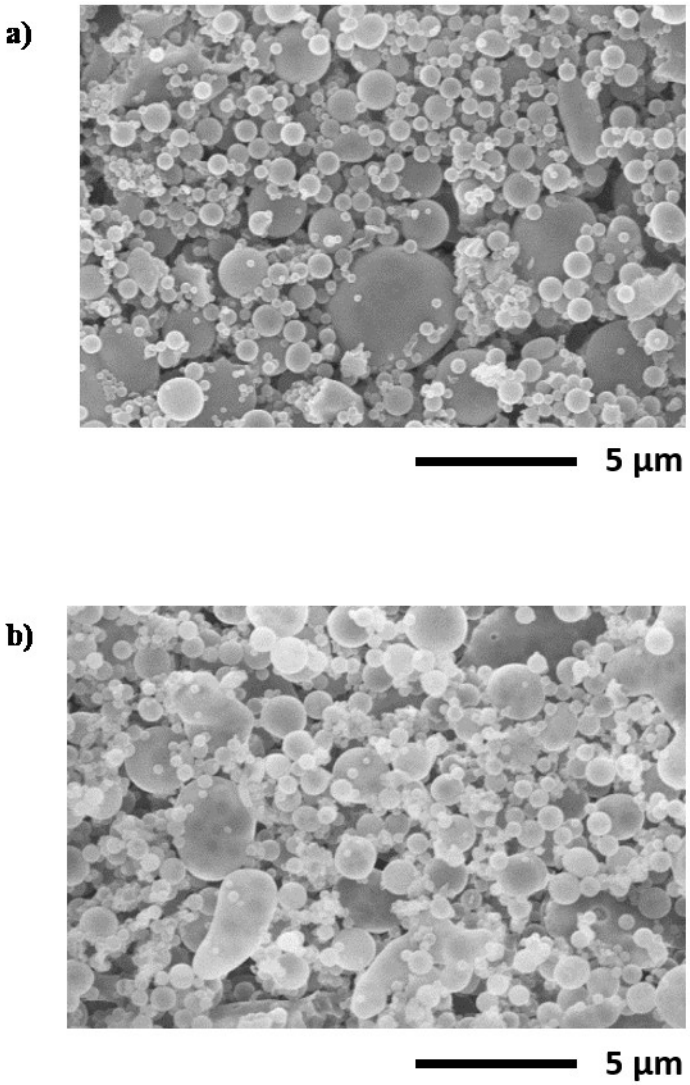

Figure 3.24 SEM images of MPs prepared at IW condition and subjected to multiple freeze drying cycles- a) after first freeze dry cycle and b) after tenth freeze dry cycle

4 Conclusion and Future Work

In efforts to develop a universal platform for combating influenza menace, the potential of pH-sensitive pored MPs as delivery vehicles was investigated in this work. All experiments were designed to include potential technical problems and future challenges associated with clinical application of MPs based vaccine. In a systematic approach, first-of-its-kind MPs with pH-responsive pores were synthesized by utilizing a modified O/W emulsion method. After successful fabrication of pored MPs, effects of temperature, solvent composition/evaporation conditions on MPs characteristics were examined to find optimal process conditions. This provided us valuable information that the solvent evaporation rate had a direct effect on the MPs properties (particle size and pores size). Control over the evaporation rate enabled us to find three potential MP conditions (i.e., 30-10-30, R.T., and IW), which have been used to characterize important characteristics of MPs such as drug encapsulation efficiency, pH responsiveness, and release behavior in simulated GI environment. In addition, the development of a novel technique to close the pores of MPs by incorporating freeze dryer increased the feasibility of MP-based oral vaccines by enhancing efficacy against the harsh acidic environment of stomach. The pores of MPs remained intact (closed) during acidic pH of stomach, but opened in the neutral pH of intestine, which was further

confirmed by monitoring release behavior of model drugs (100 nm fluorescent nanoparticles and sulforhodamine b) from MPs under simulated GI tract environment. Highly efficient release profile of drugs in MPs and precisely controlled pore opening in response to environmental pH change are critical factors to successful implementation of our proof-of-concept oral vaccine delivery using pored MPs. Although our work has been limited to the *in vitro* demonstration of the concept, the findings included in this work clearly demonstrates the potential applicability of pH-sensitive pored MPs as delivery vehicles for oral influenza vaccines. It is believed that multiple advantages of our MP-based vaccine delivery system over conventional vaccines can contribute to solving the current and future threats of deadly infectious diseases including influenza.

In terms of future plan, process parameters will be further optimized to increase MP production yield, drug encapsulation efficiency, and stability of bio pharmaceuticals during encapsulation/administration/storage. Further characterization will be carried out to investigate the stability of diverse pharmaceuticals in different form such as DNA, peptides, proteins, and whole inactivated virus vaccine. Proof-of-concept will be confirmed *in vitro* using inactivated A/PR/8/34 (H1N1) influenza A virus vaccine by measuring functional hemagglutinin activity. Lastly, *in vivo* mouse studies will be carried out to corroborate *in vitro* results.

References

(1) Mitragotri, S. *Nat. Rev. Immunol.* **2005**, *5* (12), 905–916.

(2) Samji, T. *Yale J. Biol. Med.* **2009**, *82* (4), 153–159.

(3) Fauci, A. S. *Cell* **2006**, *124* (4), 665–670.

(4) Molinari, N. a M.; Ortega-Sanchez, I. R.; Messonnier, M. L.; Thompson, W. W.; Wortley, P. M.; Weintraub, E.; Bridges, C. B. *Vaccine* **2007**, *25* (27), 5086–5096.

(5) Neumann, G.; Noda, T.; Kawaoka, Y. *Nature* **2009**, *459* (7249), 931–939.

(6) Guleria, R.; Kumar, J.; Mohan, A.; Wig, N. *Indian J. Microbiol.* **2010**, *49* (4), 315–319.

(7) HHS Pandemic Influenza Plan http://www.flu.gov/planning-preparedness/federal/hhspandemicinfluenzaplan.pdf (accessed Aug 15, 2015).

(8) Harper, S. A.; Fukuda, K.; Uyeki, T. M.; Cox, N. J.; Bridges, C. B. *MMWR. Recomm. reports Morb. Mortal. Wkly. report.* **2005**, *54* (RR-8), 1–40.

(9) Fiore, A.E.; Uyeki, T. M.; Broder, K; Finelli, L; Euler, G. L.; Singleton, J. A.; Iskander, J. K.; Wortley, P.M.; Shay, D.K.; Bresee, J.S.; Cox, N. J. *MMWR. Recomm. reports Morb. Mortal. Wkly. report.* **2010**, *59* (RR-8), 1–47.

(10) Neutra, M. R.; Kozlowski, P. a. *Nat. Rev. Immunol.* **2006**, *6* (2), 148–158.

(11) Kilbourne, E. D. *S.A. Plotkin, E.A. Mortimer, Jr. (Eds.), Vaccines, W.B. Saunders* **1988**, 420–434.

(12) Giudice, E. L.; Campbell, J. D. *Adv. Drug Deliv. Rev.* **2006**, *58* (1), 68–89.

(13) Kermode, M. *Health Promot. Int.* **2004**, *19* (1), 95–103.

(14) Talaat, M.; Kandeel, a; El-Shoubary, W.; Bodenschatz, C.; Khairy, I.; Oun, S.; Mahoney, F. J. *Am. J. Infect. Control* **2003**, *31* (8), 469–474.

(15) How Influenza (Flu) Vaccines Are Made http://www.cdc.gov/flu/protect/vaccine/how-fluvaccine-made.htm (accessed Aug 15, 2015).

(16) Huang, J.; Garmise, R. J.; Crowder, T. M.; Mar, K.; Hwang, C. R.; Hickey, A. J.; Mikszta, J. a.; Sullivan, V. J. *Vaccine* **2004**, *23* (6), 794–801.

(17) Vaccines for Pandemic Threats http://www.historyofvaccines.org/content/articles/vaccines-pandemic-threats (accessed Aug 15, 2015).

(18) Mutsch, M.; Zhou, W.; Rhodes, P.; Bopp, M.; Chen, R. T.; Linder, T.; Spyr, C.; Steffen, R. *N. Engl. J. Med.* **2004**, *350* (9), 896–903.

(19) Palese, P. *Emerg. Infect. Dis.* **2006**, *12* (1), 61–65.

(20) Azizi, A.; Kumar, A.; Diaz-Mitoma, F.; Mestecky, J. *PLoS Pathog.* **2010**, *6* (11).

(21) Farag-Mahmod, F. I.; Wyde, P. R.; Rosborough, J. P.; Six, H. R. *Vaccine* **1988**, *6* (3), 262–268.

(22) Quan, F. S.; Li, Z. N.; Kim, M. C.; Yang, D.; Compans, R. W.; Steinhauer, D. a.; Kang, S. M. *Virology* **2011**, *417* (1), 196–202.

(23) Choi, H. J.; Ebersbacher, C. F.; Kim, M. C.; Kang, S. M.; Montemagno, C. D. *PLoS One* **2013**, *8* (6).

(24) Elson, C. O.; Dertzbaugh, M. T. *Mucosal Immunol. Two-Volume Set* **2005**, *23*, 967–986.

(25) Eriksson, Kristina; Holmgren, J. *Curr. Opin. Immunol.* **2002**, *14* (5), 666–672.

(26) Sahil, K.; Akanksha, M.; Premjeet, S.; Bilandi, A.; Kapoor, B. *Int. J. Res. Pharm. Chem. Available* **2011**, *1* (4), 1184–1198.

(27) Letchford, K.; Burt, H. *Eur. J. Pharm. Biopharm.* **2007**, *65* (3), 259–269.

(28) Edlund, U.; Albertsson, A.-C. In *Advances in Polymer Science, Vol. 157*; Springer Berlin Heidelberg: Berlin, Heidelberg, 2002; pp 67–112.

(29) Wang, C.; Kang, Y.; Liu, K.; Li, Z.; Wang, Z.; Zhang, X. *Polym. Chem.* **2012**, *3* (11), 3056.

(30) Reinhardt, M.; Dzubiella, J.; Trapp, M.; Gutfreund, P.; Kreuzer, M.; Gröschel, A. H.; Müller, A. H. E.; Ballauff, M.; Steitz, R. *Macromolecules* **2013**, *46* (16), 6541–6547.

(31) Meng, H.; Mohamadian, H.; Stubblefield, M.; Jerro, D.; Ibekwe, S.; Pang, S.-S.; Li, G. *Smart Mater. Struct.* **2013**, *22* (9), 093001.

(32) Zhang, M.; Estournès, C.; Bietsch, W.; Muller, A. H. E. *Adv. Funct. Mater.* **2004**, *14* (9), 871–882.

(33) Ware, T.; Simon, D.; Rennaker, R. L.; Voit, W. *Polym. Rev.* **2013**, *53* (1), 108–129.

(34) Kikuchi, A.; Okano, T. *Prog. Polym. Sci.* **2002**, *27* (6), 1165–1193.

(35) Evans, D. F.; Pye, G.; Bramley, R.; Clark, a G.; Dyson, T. J.; Hardcastle, J. D. *Gut* **1988**, *29* (8), 1035–1041.

(36) O'Hagan, D. T. *Adv. Drug Deliv. Rev.* **1990**, *5* (3), 265–285.

(37) Eldridge, J. H.; Hammond, C. J.; Meulbroek, J. a.; Staas, J. K.; Gilley, R. M.; Tice, T. R. *J. Control. Release* **1990**, *11* (1-3), 205–214.

(38) Alonso, M. J.; Gupta, R. K.; Min, C.; Siber, G. R.; Langer, R. *Vaccine* **1994**, *12* (4), 299–306.

(39) Raghuvanshi, R. S.; Katare, Y. K.; Lalwani, K.; Ali, M. M.; Singh, O.; Panda, A. K. *Int. J. Pharm.* **2002**, *245* (1-2), 109–121.

(40) Slobbe, L.; Medlicott, N.; Lockhart, E.; Davies, N.; Tucker, I.; Razzak, M.; Buchan, G. *Immunol. Cell Biol.* **2003**, *81* (3), 185–191.

(41) Calvo, P.; Remuñan-López, C.; Vila-Jato, J. L.; Alonso, M. J. *Pharm. Res.* **1997**, *14* (10), 1431–1436.

(42) Chattaraj, S. C.; Rathinavelu, A.; Das, S. K. *J. Control. Release* **1999**, *58* (2), 223–232.

(43) O'Hagan, D. T.; Singh, M.; Gupta, R. K. *Adv. Drug Deliv. Rev.* **1998**, *32* (3), 225–246.

(44) Taylor, M. J.; Tanna, S.; Sahota, T. *J. Pharm. Sci.* **2010**, *99* (10), 4215–4227.

(45) Burgain, J.; Corgneau, M.; Scher, J.; Gaiani, C. In *Microencapsulation and Microspheres for Food Applications*; Elsevier, Ed.; Elsevier, 2015; pp 391–406.

(46) Tabata, Y.; Inoue, Y.; Ikada, Y. *Vaccine* **1996**, *14* (17-18), 1677–1685.

(47) Technical Information- EUDRAGIT® L 100 and EUDRAGIT® S 100 http://eudragit.evonik.com/sites/lists/HN/ProductSpecifications/TI-EUDRAGIT-L-100-S-100-EN.pdf (accessed Aug 15, 2015).

(48) Hyuk Im, S.; Jeong, U.; Xia, Y. *Nat. Mater.* **2005**, *4* (9), 671–675.

(49) EUDRAGIT® S 100 http://eudragit.evonik.com/product/eudragit/en/products-services/eudragit-products/enteric-formulations/s-100/Pages/default.aspx (accessed Aug 15, 2015).

(50) Raju, C. H. L.; Rao, J. L.; Reddy, B. C. V; Brahmam, K. V. *Bull. Mater. Sci.* **2007**, *30* (3), 215–218.

(51) Choi, H.; Montemagno, C. D. In *Epidemiology-theory, research and practice*; iConcept Press Ltd, 2014.